FALDI-Based Criterion for and the Origin of an Electron Density Bridge with an Associated (3,–1) Critical Point on Bader's Molecular Graph

*Jurgens H. de Lange, Daniël M.E. van Niekerk, Ignacy Cukrowski**

Correspondence to: Ignacy Cukrowski (E-mail: *ignacy.cukrowski@up.ac.za*)

Department of Chemistry, Faculty of Natural and Agricultural Sciences, University of Pretoria, Lynnwood Road, Hatfield, Pretoria 0002, South Africa

KEYWORDS:

Atomic Interaction Line, Bond path, FALDI, Chemical bond, Intramolecular interaction

Abstract

The total electron density (ED) along the λ_2-eigenvector is decomposed into contributions which either *facilitate* or *hinder* the presence of an electron density bridge (DB, often called an atomic interaction line or a bond path). Our FALDI-based approach explains a DB presence as a result of a dominating rate of change of facilitating factors relative to the rate of change of hindering factors; a novel and universal criterion for a DB presence is thus proposed. Importantly, facilitating factors show, in absolute terms, a concentration of ED in the internuclear region as commonly observed for most chemical bonds, whereas hindering factors show a depletion of ED in the internuclear region. We test our approach on four intra-molecular interactions, namely (i) an attractive classical H-bond, (ii) a repulsive O···O interaction, (iii) an attractive Cl···Cl interaction and (iv) an attractive CH···HC interaction. (Dis)appearance of a DB is (i) shown to be due to a 'small' change in molecular environment and (ii) quali- and quantitatively linked with specific atoms and atom-pairs. The protocol described is equally applicable (a) to any internuclear region, (b) regardless of what kind of interaction (attractive/repulsive) atoms are involved in, (c) at any level of theory used to compute the molecular structure and corresponding wavefunction, and (d) equilibrium or non-equilibrium structures. Finally, we argue for a paradigm shift in the description of chemical interactions, from the ED perspective, in favour of a multicenter rather than diatomic approach in interpreting ED distributions in internuclear regions.

Introduction

From a general chemist's perspective, conceptual understanding of a chemical bond is an amalgamation of various chemical bond theories, empirical observations and intuition. Existing chemical bond theories are, for the most part, deductive inferences on calculations and experiments performed on very small and simple systems. Even modern developments in the field will almost always develop from a bottom-up approach, and our conceptual understanding of a chemical bond is therefore always much clearer for di- or few-atomic molecules. As it stands, there is no general and universal theory of a chemical bond and terms such as 'chemical bonding' rather than 'a chemical bond' dominate titles of chapters in two dedicated[1,2] published recently.

Unfortunately, complexity in chemical systems scales exponentially with an increasing number of atoms and bonds, and so does the difficulty of interpreting chemical bond models. For instance, both molecular orbital (MO) and valence bond (VB) theories are simple to understand and interpret for diatomic molecules, but their interpretation becomes increasingly convoluted as the number of MOs or allowable states increase. The same problem applies to many modern theoretical and computational approaches, such as calculations of bond dissociation energy and deformation densities. One of the biggest hurdles facing chemical bond theory is that the current paradigm places immense focus on bonds as a diatomic property of a molecule, whereas the wavefunction and changes within the wavefunction occur on a molecular-wide, hence a polyatomic scale. The irreducible cornerstone of a bond – that a chemical bond requires energy to break – is usually exemplified through measurements of energy differences between an interacting and non-interacting states. Such experiments study the *process* assumed to be a single diatomic, intra- or intermolecular, bond formation and do not consider the intrinsic property of a molecule as a collection of atoms interacting simultaneously with each other. The usage and interpretation of binding energies particularly fails in the case of the interpretation of intramolecular interactions, as it always involves more than just two atoms and requires breaking multiple bonds.

Quantum Chemical Topology (QCT)[3] encompasses a range of approaches which, in principle, do not suffer from the above-mentioned complexity scaling. The most prominent QCT method is Bader's Quantum Theory of Atoms in Molecules (QTAIM).[4] QTAIM's molecular graphs – a series of electron density bridges (DBs, but also commonly called atomic interaction lines, line paths[5,6] or bond paths[7]) – are equally applicable to simple, small, large, hence complex molecules. Historically, the interpretation of a DB was associated, by induction, with a chemical bond: remarkably, a DB is observed wherever

chemists can *unanimously* agree that a chemical bond should exist. Since the first observations of the equivalence between a DB and a chemical bond,[7,8] many questions regarding the validity and universality of a DB as an indicator of a chemical bond lead to a fierce scientific discourse,[5,6,9–15] which will be discussed shortly. However, the large degree of correspondence between the presence of a DB and the general chemist's chemical bond is the impetus for continued research into the nature and interpretation of a DB. A range of properties of a DB, and specifically topological and energetic properties at the (3,–1) critical point (CP, commonly known as a bond critical point) associated with a DB, have been linked to and successfully applied in describing chemical phenomena, *e.g.*, bond strengths,[16,17] open- and closed-shell natures of interactions,[17] bond orders, degrees of π-bonding,[18] and many more.

The critique that cautions the over-interpretation of DBs, critique that has been growing steadily over the last two decades, focuses on the two cases which places doubt on the universality of the interpretation of a DB as a bond path: (i) cases where a DB is observed but no chemical bond is expected,[9–13] and (ii) cases where a chemical bond is expected but no DB is observed.[19,20] The most prominent example of the former situation is of DBs which exist between H-atoms in a wide range of molecules and lead to a long series of debates regarding the chemical nature of CH···HC interactions.[11–13,15,21,22] The existence of a DB in these and other non-conventional types of interactions, many of which can be attractive or repulsive in nature, have placed considerable doubt on the conceptual homeomorphism between QTAIM molecular graphs and the lines which chemists draw to indicate bonds. For the inverse case – where a chemical bond is expected but no DB is observed – researchers have found evidence from other descriptors, such as the Non-covalent Interactions (NCI) technique,[23,24] the source-function and delocalization indices that indicate the presence of some form of chemical interaction but it is not supported by a (3,–1) CP on a DB.[19,20] These examples further illustrate that the relationship between various theoretical approaches and the topology of the electron density (ED) is not fully understood yet. In addition, the presence or absence of DBs is often seemingly inexplicable, which adds to the ambiguity regarding the interpretation of a DB. For instance, we have previously shown[14] that the presence of a DB is strongly subjected to effects of the local environment, proving that the *nature* of an interaction might remain the same regardless of the presence or absence of a DB.

The interpretation of a DB has evolved somewhat over time as well. Originally, Bader had all but suggested that a DB and a chemical bond are synonymous.[7,8,25] Later on, he stressed that DBs are not chemical bonds, but rather represent 'bonding interactions'[15,16] – a

mechanism of the molecular ED distribution that serves to lower the molecular energy. Pendás *et al*. presented an alternative interpretation by postulating that a DB represents a 'privileged exchange channel'.[26] Their concept of a DB was further explored by Tognetti and Joubert[27,28] (TJ). TJ studied a number of intramolecular interactions where a DB was present in some but not other molecules, and investigated whether the presence of a DB could be linked with 'privileged exchange'. Their approach involved calculating the IQA-defined[29] interatomic exchange correlation (XC) energies, $V_{\mathrm{XC}}^{\mathrm{X,Y}}$, of the interaction between two atoms of interest (the '*primary interaction*') as well as neighbouring '*secondary interactions*'. They found that if the ratio, $\beta = V_{\mathrm{XC}}^{\mathrm{primary}} / V_{\mathrm{XC}}^{\mathrm{secondary}} > 1.59$ (where secondary refers to a pair of atoms for which the $V_{\mathrm{XC}}^{\mathrm{X,Y}}$ term is largest among all secondary interactions) then a DB was always present whereas for $\beta < 1.35$ no DB was observed. β-ratios between 1.35 and 1.59 were found to be ambiguous – DBs might or might not be present in this range. TJ interpreted the presence of a DB as (i) evidence of privilege in support of Pendás *et al's* ideas[26] and (ii) the primary interaction being successful in *competing against* various exchange channels of the secondary interactions. Unfortunately, the ambiguity inherent in their β-ratios suggests that either (i) not all DBs represent 'privileged exchange channels', (ii) the exclusive use of the integrated $V_{\mathrm{XC}}^{\mathrm{X,Y}}$ for just a diatomic interaction is not ideal for measuring privilege, or (iii) possibly, the concept of 'privileged exchange channels' in predicting the presence/absence of a DB is incorrect.

All previous interpretations of a DB step into the same 'trap' as for the interpretation of chemical bonds – that the interaction between atoms in a molecule can be reduced to bicentric nature (*i.e.* line structures) that is subconsciously re-enforced by DBs linking two (and only two) nuclei at a time. However, the ED (as well as critical points in the ED) is a field influenced by *all particles* of a molecule, and therefore the notion that a DB is a diatomic property is false. In fact, we have previously shown[30] that the ED at a (3,–1) CP is a result of contributions from delocalized electrons arising from multiple atoms, thereby concluding that a DB is inherently multicenter in nature even in the case of a classical covalent bond. A similar problem facing existing interpretations of a DB is the use of the second eigenvalue of the Hessian matrix as a measure of electron concentration for the fulfilment of Feynman's theorem[31] (the basis for Bader's interpretation[15,16] as well as the interpretation of other methods such as NCI[23,24]). This approach is flawed,[14] as it only measures the *local*, relative electron concentration rather than the absolute, and resultantly shows a large dependence on the local environment. Our own Fragment, Atom, Localized,

Delocalized and Interatomic (FALDI) density decomposition scheme[30,32–34] provides absolute measures of electron concentration for 1- and 2-centre ED distributions. Hence, FALDI provides a much more trustworthy measure[30] with regards to a concentration (and its origin) of ED within an internuclear region.

This work presents a new theoretical methodology that provides meaningful explanation of the presence (or absence) of a DB. Although our approach appears as simple in its final implementation, it required a paradigm shift in searching for the origin and meaning of a DB. Our approach comes from a realization that the nature of a DB is inherently not chemical, only its interpretation. Hence, the main focus should be on the ED itself and the elementary conditions required for the presence of a DB, rather than a direct link to chemical concepts such as atoms and linking them bonds. We propose here a set of topological criteria; with the gradient of the ED (along the eigenvector associated with the λ_2 eigenvalue of the Hessian matrix) determining *if* a critical point is present and the second derivative of the ED determining *which* type of critical point is present. To link the mathematics of DB presence with chemical meaning, we decompose the gradient of the ED (which in itself is difficult to interpret from a chemist's point of view) into components with clear chemical and physical interpretations. In principle, this approach can be taken with a large number of established ED decompositions. However, we have chosen our recently developed FALDI density decomposition scheme,[30,32–34] as FALDI is (i) inherently linked to QTAIM atomic basins and populations, and (ii) FALDI can provide visualisation and quantify electron exchange-correlation channels in real 3D space.

Our primary aim in this work is to derive and introduce the tools necessary to detect and explain the presence or absence of a DB. We will refrain from providing in depth and universal interpretations of a DB in terms of chemical bonding. This is because a sound interpretation of a DB should be extremely robust, general, predictive and physically and chemically meaningful – an endeavour which is not taken lightly. Rather, we will provide a general criterion for the presence of a DB in terms of the gradients of our FALDI decomposition components, culminating in an approach that we hope ourselves or others can use to understand the difficult relationship between the ED distribution and chemical bonding. We present our approach with four case studies focusing on intramolecular interactions, as possibly they represent the most difficult case for chemists to interpret. However, our approach is of general nature; it applies equally to inter- and intramolecular, weak and strong interactions. In three of the case studies, two similar molecules are investigated, and in each system a non-local perturbation results in the appearance of a DB

linking atoms involved in an interaction of interest. Our case studies include an attractive intramolecular H-bond, a repulsive O···O interaction, an attractive Cl···Cl interaction and lastly, an attractive CH···HC interaction.

Theoretical Background

A critical point (CP) in the ED at a coordinate $\mathbf{r}_c$ is a local maximum, minimum or a saddle point where the first derivative, and each of its three components, vanish:[4]

$$\nabla\rho(\mathbf{r}_c) = \mathbf{i}\frac{\partial\rho}{\partial x} + \mathbf{j}\frac{\partial\rho}{\partial x} + \mathbf{k}\frac{\partial\rho}{\partial z} = 0 \qquad (1)$$

The unit vectors in Eq. 1 are the principle axes at $\mathbf{r}_c$, and are determined by the eigenvectors of the matrix of partial second derivatives (the Hessian matrix) of the ED at $\mathbf{r}_c$. The type of CP can be determined by evaluating the eigenvalues (λ_1, λ_2 and λ_3) of the Hessian matrix. A CP found wherever a DB is present is a local minimum along one of the axes and local maxima along the other two axes, labeled as (+3,–1), where the *rank* (+3) denotes the number of non-zero eigenvalues at $\mathbf{r}_c$ and the *signature* (–1) is the algebraic sum of the signs of the eigenvalues. A (+3,–1) CP has historically been called a number of names, from Bader's original bond critical point[4] to more recent line or edge critical point.[5,6] In this work, we will only refer to this CP as (3,–1) CP in order to reduce as much secondary and implied meanings as possible. For the case of a (3,–1) CP, λ_1 and λ_2 are negative (local maxima) whereas λ_3 is positive (local minimum) and, by convention, $\lambda_1 \leq \lambda_2 \leq \lambda_3$. A CP close to a nucleus is a (+3,–3) CP (a local maximum along all three axes) where all eigenvalues are negative. Therefore, in an interatomic region between two nuclei, λ_3 will always be positive, corresponding to a region of local minimum ED along the internuclear vector. Furthermore, unless the two nuclei are part of a cage, λ_1 will always be negative, corresponding to a local maximum along one of the axes perpendicular to the internuclear vector. The sign of the remaining eigenvalue, λ_2, corresponding to the other perpendicular axis, determines whether the CP is of (3,–1) ($\lambda_2 < 0$, a local maximum) or a (3,+1) ($\lambda_2 > 0$, a local minimum), also called a ring critical point. The sign of λ_2 therefore contains very valuable information regarding the nature of the CP at $\mathbf{r}_c$. In addition, the second derivative of the ED is a measure of density concentration ($\nabla^2\rho(\mathbf{r}) < 0$) or depletion ($\nabla^2\rho(\mathbf{r}) > 0$). At any coordinate of a DB the ED is therefore depleted along the internuclear vector ($\lambda_3 > 0$) but concentrated along all perpendicular vectors ($\lambda_1 < 0$, $\lambda_2 < 0$). It is for this reason that a DB is often called a 'bridge of density'.[15]

A DB will always exist if an associated (3,–1) CP is present, and therefore it is enough to investigate when such a CP may (or may not) be present. Since the presence of a CP depends on the gradient of the ED rather than the ED itself or components of its second derivative, it is important to understand the directional first derivatives of the ED along principle axes in an internuclear region in both the presence and absence of a (3,–1) CP. Note that all derivatives – including components of the Hessian matrix as well as its eigenvalues and eigenvectors – can be calculated at any coordinate **r** regardless of whether a critical point is present at **r** or not. A local minimum in the ED along the internuclear vector is always present between two (3,–3) CPs of atomic basins that share an interatomic surface. Hence, the directional derivative of the ED along the internuclear vector will always vanish at some coordinate (corresponding to a local minimum in the ED) regardless of the presence or absence of a (3,–1) CP. Generally, the principle axis along which this derivative vanishes is the direction of the eigenvector associated with λ_3. We label such a local minimum on the internuclear vector as a geometric *minimum density point* (MDP, previously also called a geometric interaction point[14]). The internuclear vector, an MDP and the directions of all three eigenvectors of the Hessian matrix at the MDP are shown, as an illustrative example, for the internuclear region between two H-atoms in close contact (*i.e.* H1 and H6) in *cis*-2-butene in Figure 1. *Cis*-2-butene was selected because three topological points (MDP, (3,–1) CP and (3, +1) CP) are well-separated on the molecular graph – Figure 1(a). Figure 1(b) shows the ED along the internuclear vector, clearly illustrating the local minimum and demonstrates how an MDP can easily be found. The perpendicular principle axes at the MDP correspond to the directions of the eigenvectors associated with λ_1 and λ_2. As mentioned above, λ_1 is usually negative unless the internuclear region is part of a cage and, in most cases, the local maximum is observed as shown in Figure 1(c); hence, directional derivative along the λ_1-eigenvector at MDP will vanish. That leaves the directional derivative along the 2nd eigenvector of the Hessian matrix as the deciding factor for the presence or absence of most (3,–1) CPs. If this derivative vanishes, due to a local maximum in the ED along the 2nd eigenvector – Figure 1(d), then the slope of the ED will be zero and a (3,–1) CP will be present. If this derivative does not vanish, then a (3,–1) CP will be absent regardless of the fact that the ED at the MDP is a local maximum and minimum along the directions of the 1st and 3rd eigenvectors of the Hessian matrix, respectively. Hence, in order to understand when a DB may be present between two atoms that share an interatomic surface, the components of the slope of the ED along the principle axis λ_2 in the interatomic region should be investigated.

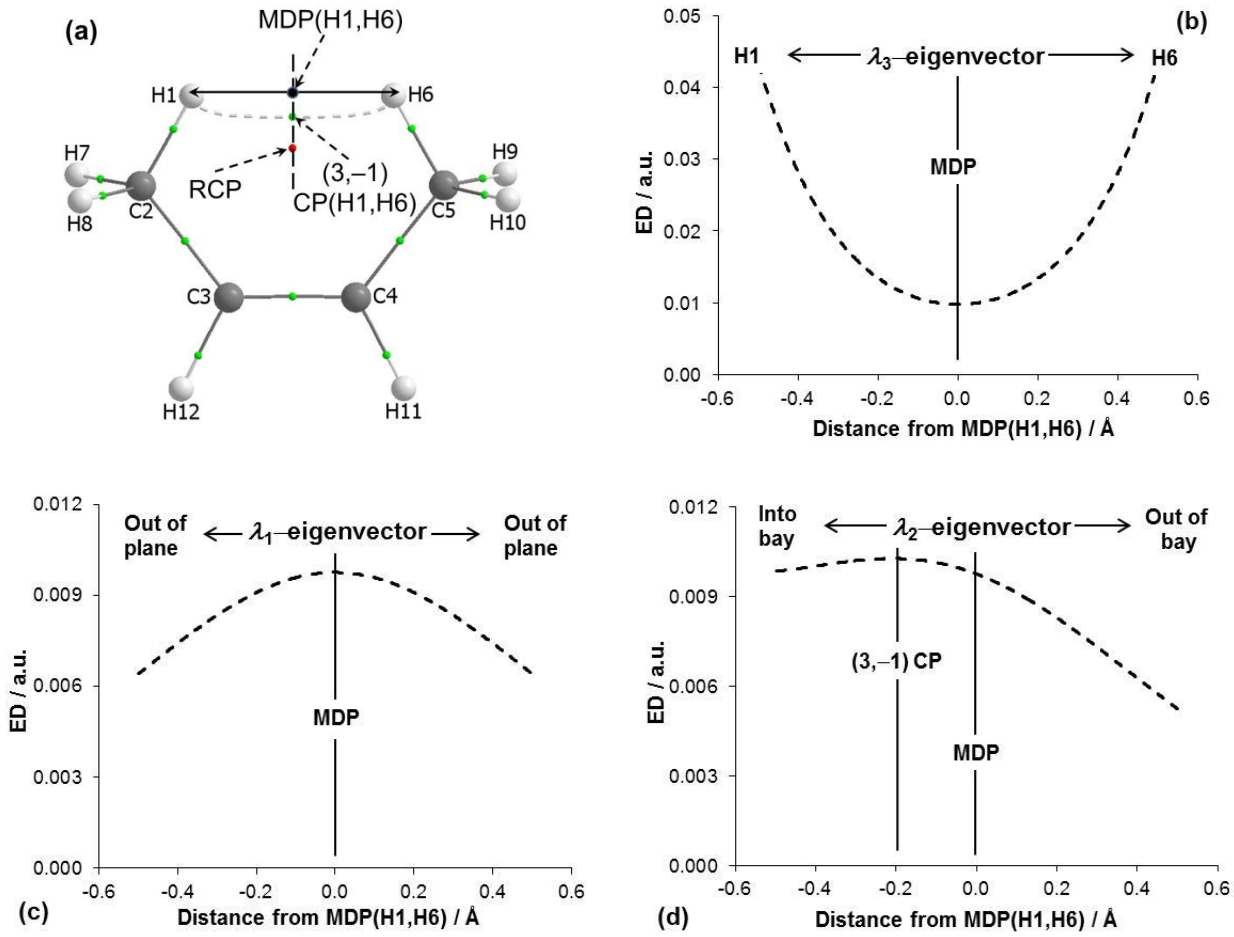

Figure 1. Part (a) - a molecular graph of *cis*-2-butene showing a (3,–1) CP as a small green sphere on a density bridge between H1 and H6 atoms, RCP = (3,+1) CP as a small red sphere, and a minimum density point (MDP) on line geometrically linking 3D-coordinates of H1 and H6 nuclei. Part (b) - the total ED computed along the λ_3-eigenvector (a line geometrically linking 3D-coordinates of H1 and H6 nuclei) with the MDP located at the minimum. Part (c) – variation in the total ED along the λ_1-eigenvector. Part (d) – variation in the total ED along the λ_2-eigenvector also showing locations of the (3,–1) CP (at the maximum of ED) and MDP.

In a diatomic molecule, the slope of the ED along the eigenvector associated with λ_2 (henceforth referred to as the λ_2–eigenvector) will always vanish at some **r** on the internuclear vector, hence a DB and (3,–1) CP will always be present. However, in the presence of other (3,–1) CPs (in any polyatomic molecule), the slope of the ED along the λ_2–eigenvector is not guaranteed to vanish, and thus a (3,–1) CP will not be present between every nuclear pair. The presence of such CPs in polyatomic molecules depends on the environment. Typically, a strong interaction (such as a covalent bond) contains highly concentrated ED perpendicular to the internuclear vector, and a (3,–1) CP exists despite the presence of factors that hinder its presence. On the other hand, weak interactions (such as an intramolecular H-bond) have significantly less concentrated ED perpendicular to the

internuclear vector, and a (3,–1) CP will only appear if the environment is favorable (*i.e*. in the absence of dominating factors which topologically hinder the presence of a (3,–1) CP). Regrettably, the precise chemical conditions required to foretell the presence of a (3,–1) CP (particularly for weak interactions) are not yet known exactly, despite previous attempts,[27,28] and therefore the chemical significance of a DB is difficult to determine.

The slope of the ED along the λ_2–eigenvector is an exact predictor for the existence of a (3,–1) CP and is easy to measure in most systems. In order to determine when a (3,–1) CP may form from a chemical point of view, however, one must understand first the physical factors which lead to a given ED distribution. To achieve that, the ED must be decomposed along the λ_2–eigenvector into chemically and physically meaningful components in order to understand the ED distribution on a fundamental level. Specifically, provided that the contribution made to the total ED (*tot-ED*) by a primary interaction as well as by all other ones can be quantified, then it should be possible to determine whether a (3,–1) CP will exist in a given environment based on criteria other than the topology of the *tot*-ED. Subsequently, the components giving rise to a (3,–1) CP could then be scrutinized analytically in order to understand why the CP exists. Finally, if and only when the components themselves carry chemical significance, such information could be useful in determining the chemical conditions necessary for the existence of a (3,–1) CP and, therefore, a presence of a DB could be meaningfully interpreted in terms of chemical bonding.

We present in this work a scheme that determines components of the molecular system *tot*-ED that either facilitate or hinder the presence of a (3,–1) CP in the interatomic region of an interaction of interest. We also measure the exact contribution made by each component to arrive at a criterion which explains the presence or absence of a (3,–1) CP. We first describe a suitable *tot*-ED decomposition technique, followed by a classification scheme which determines whether a decomposition component facilitates or hinders the presence of a DB, and finally we introduce an index to condense the information.

The FALDI density decomposition scheme

We recently introduced the Fragment, Atomic, Localized, Delocalized and Interatomic (FALDI) ED decomposition scheme.[30,32,34] FALDI uses concepts from the Domain Averaged Fermi Hole (DAFH)[35,36] approach in order to calculate pseudo-2nd order contributions arising from electrons within QTAIM-defined atomic basins. FALDI decomposes the *tot*-ED at any coordinate **r** into 1- and 2-centre contributions:

$$\rho(\mathbf{r}) = \sum_{\mathrm{A}}^{M} \mathcal{L}_{\mathrm{A}}(\mathbf{r}) + \sum_{\mathrm{A}}^{M-1} \sum_{\mathrm{B=A+1}}^{M} \mathcal{D}_{\mathrm{A,B}}(\mathbf{r}) \tag{2}$$

where M is the number of QTAIM-defined atomic basins. $\mathcal{L}_{\mathrm{A}}(\mathbf{r})$ is known as a 1-centre localized ED (*loc*–ED) distribution, and describes the ED that is localized *exclusively* within an atomic basin Ω_{A}, as shown in Eq. 3,

$$\mathcal{L}_{\mathrm{A}}(\mathbf{r}) = \sum_{i}^{N} \mathrm{n}_i''^{\mathrm{AA}} \left[\phi_i^{\mathrm{AA}}(\mathbf{r})\right]^2 \tag{3}$$

where N is the number of MOs, $\phi_i^{\mathrm{AA}}(\mathbf{r})$ is a natural density function (NDF) obtained by diagonalizing the product of the atomic overlap matrices, $\mathbf{S}^{\mathrm{A}}\mathbf{S}^{\mathrm{A}}$, and $\mathrm{n}_i''^{\mathrm{AA}}$ is the occupation of the associated NDF; it is double-primed to indicate that it is free of any localized-delocalized overlap, as previously described.[34] $\mathcal{D}_{\mathrm{A,B}}(\mathbf{r})$ is a 2-centre delocalized ED (*deloc*–ED) distribution, and describes the ED that is delocalized between the atomic basins Ω_{A} and Ω_{B}:

$$\mathcal{D}_{\mathrm{A,B}}(\mathbf{r}) = \sum_{j}^{N} \mathrm{n}_j''^{\mathrm{AB}} \left[\phi_j^{\mathrm{AB}}(\mathbf{r})\right]^2 + \sum_{j}^{N}\sum_{i}^{N} \left\{ n''(\mathcal{L}_{\mathrm{A}}^{i} \rightarrow \mathcal{D}_{\mathrm{A,B}}^{j}) \left[\phi_i^{\mathrm{AA}}(\mathbf{r})\right]^2 + n''(\mathcal{L}_{\mathrm{B}}^{i} \rightarrow \mathcal{D}_{\mathrm{A,B}}^{j}) \left[\phi_i^{\mathrm{BB}}(\mathbf{r})\right]^2 \right\} \tag{4}$$

where $\phi_j^{\mathrm{AB}}(\mathbf{r})$ is an NDF obtained by diagonalizing the product of atomic overlap matrices, $\mathbf{S}^{\mathrm{A}}\mathbf{S}^{\mathrm{B}}$, and $\mathcal{D}_{\mathrm{A,B}}(\mathbf{r})$ is corrected in the second term of Eq. 4 by any overlap that it has with NDFs of associated *loc*–ED (Eq. 3). Specifically, the degree of overlap the *i*th NDF of a *loc*–ED distribution ($\mathcal{L}_{\mathrm{A}}^{i}$) has with the *j*th NDF of a *deloc*–ED distribution ($\mathcal{D}_{\mathrm{A,B}}^{j}$) is calculated by the function $n''(\mathcal{L}_{\mathrm{A}}^{i} \rightarrow \mathcal{D}_{\mathrm{A,B}}^{j})$, which relates the relative overlap between $\mathcal{L}_{\mathrm{A}}^{i}$ and $\mathcal{D}_{\mathrm{A,B}}^{j}$ to the total overlap of $\mathcal{L}_{\mathrm{A}}^{i}$ with the remainder of the molecule's NDFs, as detailed in our previous work.[34]

From the particular ED decomposition expressed by Eq. 2 it follows that the *loc*–ED distributions describe the core (not shared) electrons of each atomic basin while the *deloc*–ED distributions then describe the electrons shared between two atoms (corresponding to valence electrons of the two atomic basins). Integrating *loc*–ED and *deloc*–ED distributions over all molecular space yields the associated exclusive localization and delocalization indices ($\mathrm{LI}_{\mathrm{excl}}$ and $\mathrm{DI}_{\mathrm{excl}}$); these distributions are similar to orthodox QTAIM (de)localization indices but intentionally designed to be free of any mutual overlap between *loc*–ED and *deloc*–ED distributions. To this effect, *e.g.*, in ethane (i) the *loc*–ED for each carbon atom describes the core 1*s* ED; it yields exactly 2 electrons when integrated over entire molecular

space, and (2) the *deloc*–ED for the two carbon atoms describes the σ-bond ED shared between them (yielding exactly 2 electrons when integrated over molecular space).

We have previously used FALDI *loc*–ED and *deloc*–ED distributions for calculating deformation densities,[32,33] multicenter interactions[30] as well as re-evaluating QTAIM-based localization and delocalization indices.[34] Eq. 2 therefore provides a complete decomposition, at any coordinate, of the 1-centre contributions from each atom as well as the 2-centre contributions from each atom-pair.

Classification scheme for ED components

We previously described a classification scheme for each *deloc*–ED contribution relative to **r**.[30] We have expanded the scheme for the purposes of this study as it was necessary to also account for *loc*–ED contributions.

Firstly, let us define a specific coordinate of interest, **r***: (i) if a (3,–1) CP is present with associated a DB linking the nuclei of the interaction under investigation, then **r*** = $\mathbf{r}_c$, and (ii) when a (3,–1) CP, hence also a DB, are absent, then we set **r*** to be the position of the MDP. The MDP is used as it is at specific coordinates that are well-defined for any atom-pair sharing an interatomic surface, regardless of the presence or absence of a (3,–1) CP. We would also like to make it clear and stress that these two points, MDP and (3,–1) CP, belong to distinctively different paths: (i) MDP is located at a density minimum along a geometric straight (hence shortest) line linking two nuclei and (ii) (3,–1) CP is located on a real and physical DB (experimental observable) that links two nuclei. It is for this reason why we also would rather not use the term 'line critical point' to describe (3,–1) CPs, as it intuitively indicates the MDP rather than the CP. We also recommend to exclusively use the MDP at **r*** in experiments where the geometry is continuously perturbed in order to avoid discontinuities when a (3,–1) CP (dis)appears.

Each FALDI component (any particular *loc*–ED or *deloc*–ED distribution) can then be classified at **r*** according to its sign as well as the sign of its partial second derivative along the λ_2–eigenvector. Specifically, if a FALDI component concentrates ED along the λ_2–eigenvector in the vicinity of **r*** (implying negative partial second derivative), it facilitates the presence of a (3,–1) CP and can be said to be of a *bonding nature* (*bonding*-ED). On the other hand, if a FALDI component depletes ED along the λ_2–eigenvector in the vicinity of **r*** (positive partial second derivative applies), it hinders the presence of a (3,–1) CP and can be said to be of a *nonbonding nature* (*nonbonding*-ED). Note that the sign of the component itself is positive, regardless of a bonding or nonbonding nature. It is important to note,

however, that FALDI components can also be negative due to deconstructive interference of molecular orbitals. Accordingly, these components are labeled as *antibonding* regardless of the sign of the partial second derivative (*antibonding*-ED). Antibonding components can either facilitate or hinder the presence of a (3,–1) CP (in terms of topology), but regardless, these distributions decrease the amount of ED in the region of interest.

From the above it follows that each FALDI component can be classified as bonding, nonbonding or antibonding at any coordinate **r**. Therefore, a FALDI component can be bonding in one region (such as the *deloc*–ED of two covalently bonded carbon atoms within their internuclear space) but nonbonding in another (such as in the internuclear space of a different nearby interaction, or a pair of atoms). For the purpose of the present work, we classify each FALDI component in terms of their topologies relative to **r***, *i.e*., at the (3,–1) CP or MDP of interest. Hence, the decomposition of the *tot*-ED (Eq. 2) at a (3,–1) CP or MDP can therefore be rewritten as:

$$\rho(\mathbf{r^*}) = \rho_{\text{bonding}}(\mathbf{r^*}) + \rho_{\text{nonbonding}}(\mathbf{r^*}) + \rho_{\text{antibonding}}(\mathbf{r^*}) \qquad (5)$$

The decomposition of the gradient in bonding, nonbonding and antibonding terms

While the above classification pertains to the sign of the second derivative of a FALDI component at **r***, it is obvious that the presence or absence of a (3,–1) CP is solely related to the gradient of the *tot*-ED at the vicinity of **r***. As mentioned above, the gradient of the *tot*-ED along the λ_2–eigenvector vanishes at **r*** when a (3,–1) CP is present. To achieve our goal and understand the chemical (physical) conditions necessary for the existence of a (3,–1) CP, one must re-write the gradient (Eq. 1) in terms of the bonding, nonbonding and antibonding classification discussed in details above (Eq. 5):

$$\partial\rho(\mathbf{r^*}) = \partial\rho_{\text{bonding}}(\mathbf{r^*}) + \partial\rho_{\text{nonbonding}}(\mathbf{r^*}) + \partial\rho_{\text{antibonding}}(\mathbf{r^*}) \qquad (6)$$

Although it is obvious, we want to make it absolutely clear that for a (3,–1) CP to be present, the sum of the terms in Eq. 6 must be zero.

From our experience it follows that antibonding distributions and their slopes at a MDP or (3,–1) CP are generally very small; hence, we will ignore the effects of their contributions for the moment. Eq. 4 then reduces to the sum of the rates of changes in just the *bonding*- and *nonbonding*-EDs along the λ_2–eigenvector. In such a case, for a (3,–1) CP to be present, these two terms must be equal but have opposite sign at **r*** to meet the $\partial\rho(\mathrm{r}^*) = 0$ requirement. However, the partial second derivatives of the *bonding*- and *nonbonding*-EDs are always

negative and positive, respectively. Therefore, due to the partial second derivative of the *tot*-ED being negative ($\lambda_2 < 0$) the following must hold: (i) the absolute slope of the sum (total) of all *bonding*-ED contributions must be greater than the absolute slope of the sum (total) of *nonbonding*-ED contributions in the vicinity of a (3,–1) CP ($\left|\partial\rho_{\text{bonding}}\right| > \left|\partial\rho_{\text{nonbonding}}\right|$) and (ii) exactly at the (3,–1) CP, $\left|\partial\rho_{\text{bonding}}\right| - \left|\partial\rho_{\text{nonbonding}}\right| = 0$. As such, a complex interplay takes place between the two components in the inward and outward directions making an interpretation a bit awkward. To ease and aid the interpretation of *bonding*- and *nonbonding*-ED we propose the following $CP(\mathbf{r})$ function for detecting DBs when measured along the λ_2-eigenvector:

$$CP(\mathbf{r}) = -sign(\partial\rho_{\text{nonbonding}}(\mathbf{r}))\left[\partial\rho_{\text{bonding}}(\mathbf{r}) + \partial\rho_{\text{nonbonding}}(\mathbf{r}) + \partial\rho_{\text{antibonding}}(\mathbf{r})\right] \qquad (7)$$

The $CP(\mathbf{r})$ function returns the slope of the *tot*-ED, but with an adjusted sign depending on the sign of the slope of the *nonbonding*-ED contribution. Since the sign of the directional derivative depends on the direction in which it is measured, the $-sign(\partial\rho_{\text{nonbonding}}(\mathbf{r}))$ factor is used in order to enforce the $CP(\mathbf{r})$ function to be negative throughout *except* for regions where the sum of the gradients $\partial\rho_{\text{bonding}}(\mathbf{r})$ and $\partial\rho_{\text{antibonding}}(\mathbf{r})$ is (i) greater, in absolute value, than $\partial\rho_{\text{nonbonding}}(\mathbf{r})$ and (ii) has an opposite sign than $\partial\rho_{\text{nonbonding}}(\mathbf{r})$. Furthermore, like the slope of the *tot*-ED, the $CP(\mathbf{r}^*)$ function is equal to zero at a (3,–1) CP. However, there will always be a region along the λ_2–eigenvector close to a (3,–1) CP where $CP(\mathbf{r})$ is positive, in one or both directions. By contrast, in the absence of a (3,–1) CP, $CP(\mathbf{r})$ will be negative throughout.

As an example, consider two hypothetical distributions in Figure 2, displaying *bonding*- and *nonbonding*-ED distributions in a system with a (3,–1) CP either present (part a) or absent (part b). In both Figures 2(a) and 2(b) a region exists where the gradient of *bonding*-ED is opposite in sign than the gradient of *nonbonding*-ED. Figure 1(a) illustrates a region where the $CP(\mathbf{r})$ function is positive, however, due to a larger magnitude of *bonding*-ED than *nonbonding*-ED gradient. When a (3,–1) CP is absent (Figure 2(b)), the $CP(\mathbf{r})$ function is negative throughout because the *bonding*-ED gradient is smaller in magnitude than the *nonbonding*-ED gradient.

Note that in this hypothetical example, the total gradient (not shown in Figure 2) and the $CP(\mathbf{r})$ function (dotted line in Figure 2) are identical; however, more complex systems can be found where this is not the case. In addition, the $CP(\mathbf{r})$ function remains the same regardless of the direction in which the gradient is measured. The $CP(\mathbf{r})$ function therefore provides an additional criterion for the existence of a DB: if $CP(\mathbf{r})$ is positive anywhere on the λ_2-

eigenvector for a given internuclear region, then a (3,–1) CP as well as a DB will be present. Note that in the case of an intramolecular interaction, the presence of (3,–1) CP must be accompanied by a (3,+1) CP (commonly called a ring CP) and $CP(\mathbf{r}) > 0$ will be observed between these two CPs as shown in Figure 1(a). Furthermore, the $CP(\mathbf{r})$ function is only well-defined in a region along the λ_2–eigenvector where the directional first derivative of the total *nonbonding*–ED does not change sign, which would indicate a different nature of some of the components of the *nonbonding*–ED distribution relative to an internuclear region other than the region of interest.

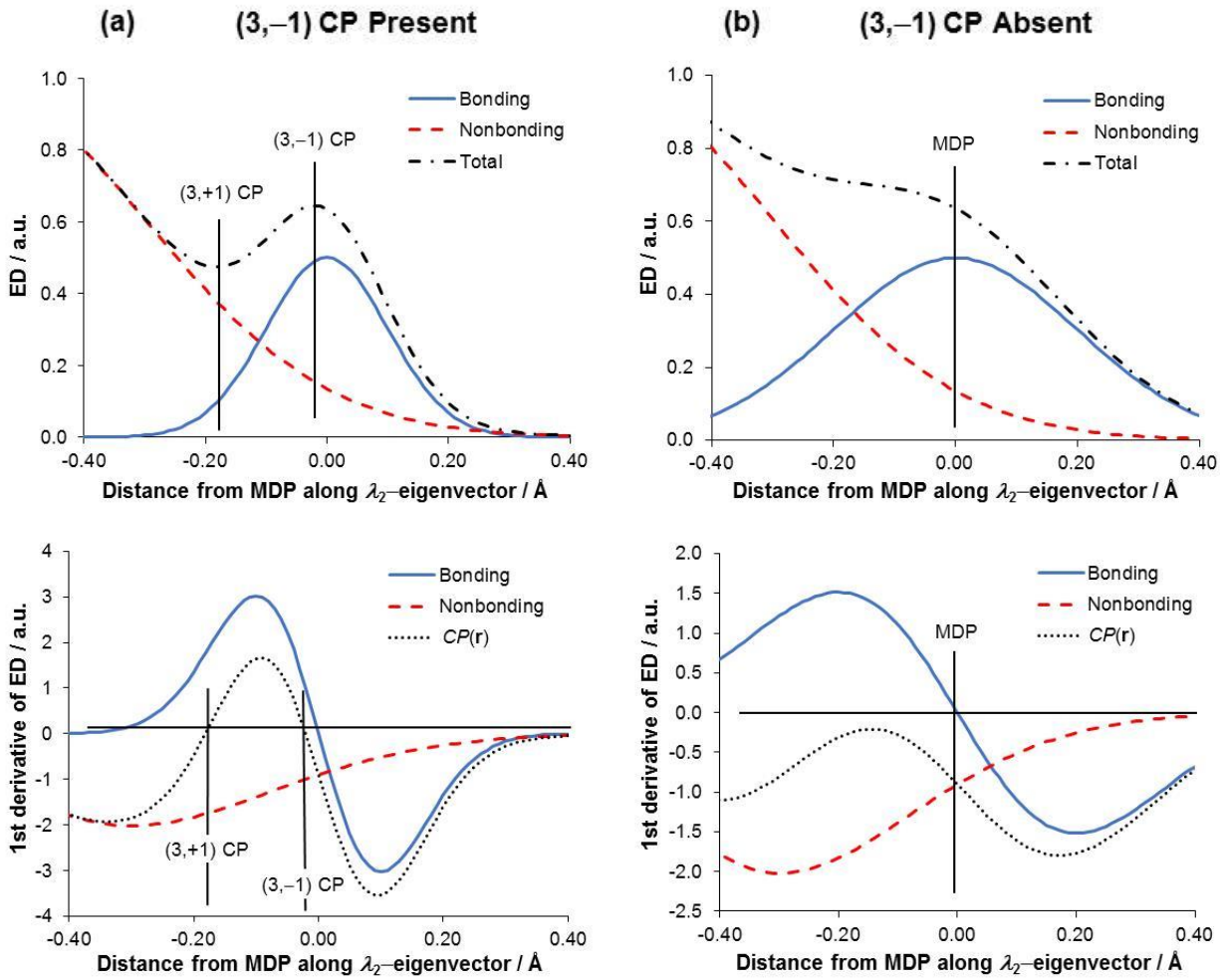

Figure 2. Hypothetical ED distributions showing *bonding*- and *nonbonding*-ED distributions as well as their gradients resulting in the presence (part a) or absence (part b) of the (3,–1) CP.

Clearly, the presence of a DB, and the associated (3,–1) CP, is an interplay between facilitating and hindering factors; to gain an insight on the origin of these factors, each term in Eq. 7 can be decomposed into individual FALDI components, such as the valence ED delocalized across two atomic basins or the core ED localized to a particular atomic basin. Doing so reveals exactly which atoms or atom-pair interactions are important towards the

presence of a DB, or which atoms and interactions hinder the presence of a DB. To this end the often-times strange presence of a DB can be investigated at a fundamental level, and the physical and chemical significance of a DB can be studied much more efficiently than in the past.

Physical and chemical interpretations of FALDI components

While the *CP*(**r**) function (as well as further decomposition) can be used to understand the interplay of various 1- and 2-centre contributions towards the presence of a DB, it will gain significantly more value when various decomposition terms are interpreted in a meaningful manner. The decomposition of ED at any coordinate **r** into *bonding*-, *nonbonding*- and *antibonding*-ED contributions (Eq. 5) can be interpreted from both physical and chemical points of view. Below, we present interpretations that can be inferred from the mathematical derivation of FALDI; however, like all interpretations of mathematical formulae, these can (and should be) thoroughly tested, refined and generalized before they can be accepted as universal interpretations of FALDI fields. We nevertheless present these interpretations as suggestions towards a better understanding of ED distributions pertaining to chemical interactions.

Physically, each term of Eq. 5 represents a measure of the absolute concentration, depletion or reduction of various FALDI components (1- and 2-centre) along the λ_2–eigenvector. *Bonding*-ED distributions contain all the FALDI components that (i) increase and (ii) *concentrate* the *tot*-ED at **r**. Concentration of ED can be viewed in terms of Feynman's theorem,[31] as explored by Bader:[15,16] a concentration of ED can maximize the attractive forces acting on a nuclei, thereby facilitating a "bonding interaction". The use of the FALDI decomposition removes the dependency of the second partial derivative of the Hessian matrix on its local environment – each FALDI component is measured absolutely relative only to itself. In contrast, *nonbonding*-ED distributions contain all the FALDI components that (i) increase, but (ii) *deplete* the *tot*-ED at **r**, thereby hindering the attractive forces acting on nuclei. Finally, *antibonding*-ED distributions always reduce the *tot*-ED at **r**.

Chemically, each term of Eq. 5 can be interpreted in terms of MO overlap. The FALDI components are derived from the overlap of all MOs and MO pairs simultaneously across atomic basins at any coordinate **r**. *Bonding*-ED distributions arise from MOs or MO pairs overlapping a single basin (in the case of *loc*–ED distributions) or simultaneously overlapping two basins (in the case of *deloc*–ED distributions) in a constructive fashion, thereby increasing and concentrating ED at **r**. In orthodox MO bond theory, such phenomena

can be linked with chemical bonding in model systems. *Nonbonding*-ED distributions, on the other hand, describe MOs or MO-pairs overlapping in a non-constructive fashion, thereby reducing the concentration of ED at **r**. Finally, *antibonding*-ED distributions describe MOs or MO-pairs that interfere deconstructively at **r**, thereby reducing the *tot*-ED.

Clearly, each FALDI component can therefore be interpreted from both physical and chemical points of view. From a physical point of view, a DB can be linked to a larger rate of change of 1- and 2-centre components that concentrate ED (and therefore maximize the forces acting on nuclei) in the internuclear region. From a chemical point of view, a DB can be linked to a larger rate of change of MOs that simultaneously overlap one and two atomic basins in a constructive fashion. While these interpretations are only aspects of chemical bonding, they can be used to investigate the properties of ED distributions in multicenter chemical interactions in a descriptive manner. We will explore the utility of these interpretations for the four case studies throughout the results section.

Computational Details

All structures were optimized in Gaussian 09, Rev. D.,[37] using B3LYP with Grimme's D3 empirical dispersion[38] with 6-311++G(d,p) in the gas phase. QTAIM molecular graphs, as well as atomic overlap matrices, were calculated using AIMAll v. 16.10.31.[39] FALDI data was calculated using in-house software, and FALDI isosurfaces were visualized using VMD.[40] Tables of cartesian coordinates for all optimized structures are given in Section 1 of the supplementary information (SI).

Results and discussion

To link our study with work by TJ,[27,28] we will use their term of '*primary interaction*' that refers to an interaction of an atom-pair of interest. TJ defined a '*secondary interaction*' as a neighbouring interaction between one of the atoms involved in the primary interaction and an atom that is linked by a DB to the second atom involved in the primary interaction. Secondary interactions in TJ's approach are seen as '*competing*' against the presence of a DB between the nuclei of the primary interaction. The secondary interaction with the largest absolute interatomic XC energy is then used for calculating TJ's β-ratio. Due to the holistic nature of our approach, we consider *all* interactions in our analysis, including the primary, secondary and all other atom-pairs. In addition, unlike TJ, we consider the possibility that any of the primary, secondary and other interactions can facilitate or hinder the presence of a DB. Furthermore, all molecular structures are presented as molecular graphs to illustrate the presence or absence of a DB between atoms of the primary interaction.

H-bonding interaction in neutral and protonated ethylenediamine

Figure 3 shows that a DB between atoms N7 and H11 (primary interaction investigated) is present only in the protonated ethylenediamine (**2**) even though d(N7,H11) < {sum of van der Waals (vdW) radii, N = 1.55 Å, H = 1.20 Å}[41] in both equilibrium structures with d(N7,H11) = 2.5893 and 1.9912 Å in structure (**1**) and (**2**), respectively.

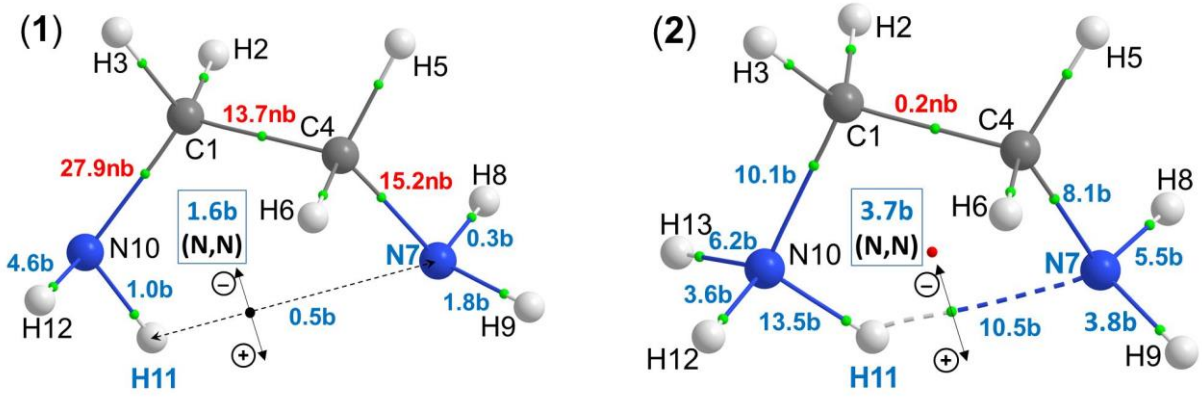

Figure 3. Molecular graphs of equilibrium structures of a neutral (**1**) and a protonated (**2**) ethylenediamine also showing the directions of λ_2–eigenvectors crossing either the minimum density point (black small sphere in (**1**)) or (3,–1) CP on density bridge (green small sphere in (**2**)). Percentage-slope contributions made by atom-pairs that facilitate and hinder the presence of a DB(N7,H11) are shown as of bonding (b) and non-bonding (nb) nature, respectively.

From the IQA perspective, there is no qualitative difference in the nature of the primary interaction in both structures; atoms H11 and N7 are involved in highly attractive interactions ($E_{\text{int}}^{\text{N7,H11}}$ = –46.6 and –104.3 kcal/mol in (**1**) and (**2**), respectively) that are predominantly of an ionic nature.

The computed TJ's β-ratios,[27,28] $V_{\text{XC}}^{\text{N7,H11}}/V_{\text{XC}}^{\text{N7,N10}}$ of (–3.16)/(–3.62) = 0.87 for (**1**) and (–16.7)/(–9.1) = 1.84 for (**2**), not only predict the absence of a DB in (**1**) correctly, but also are within the respective ranges, namely: no DB for $\beta < 1.35$ and DB present for $\beta > 1.59$. The FALDI-based decomposition of the *tot*-ED along the λ_2–eigenvectors passing through the MDP(N7,H11) in (**1**) and (3,–1) CP(N7,H11) in (**2**) (Figure 3) yields the distributions of total *bonding*- and *nonbonding*-EDs shown in Figure 4. We note that (i) qualitatively trends are similar in both structures and, focusing on values at MDP(N7,H11) in (**1**) and (3,–1) CP(N7,H11) in (**2**), (ii) the amount of *tot*-ED, *bonding*-ED as well as the ratio of *bonding*-ED/*nonbonding*-ED are always larger in (**2**) where a DB(N7,H11) is observed.

It is quite clear from the shapes of the *tot*-ED distributions in Figure 4 that a (3,–1) CP (and therefore a DB) is present in (**2**) but absent in (**1**), providing a good opportunity to explore the use of our *CP*(**r**) function. We note again that there are no *antibonding*-ED

contributions present anywhere on the λ_2-eigenvectors of (**1**) and (**2**), as for all structures studied in this work.

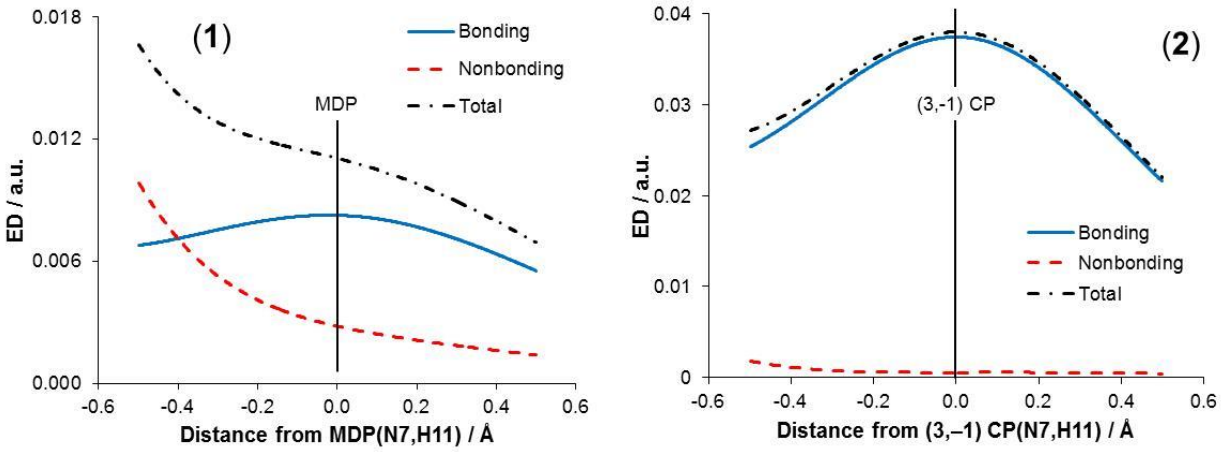

Figure 4. The *tot*-ED as well as the total *bonding*- and *nonbonding*-ED components computed along the λ_2–eigenvector passing through the MDP(N7,H11) in (**1**) and (3,–1) CP(N7,H11) in (**2**).

It is immediately seen in Figure 5 that the *CP*(**r**) function (dotted line) is negative in the entire region in (**1**), hence no DB is present, whereas it is positive in the inward region and zero at **r*** – the position of the (3,–1) CP(N7,H11) where the change in *bonding*- and *nonbonding*-ED is opposite but equal in value.

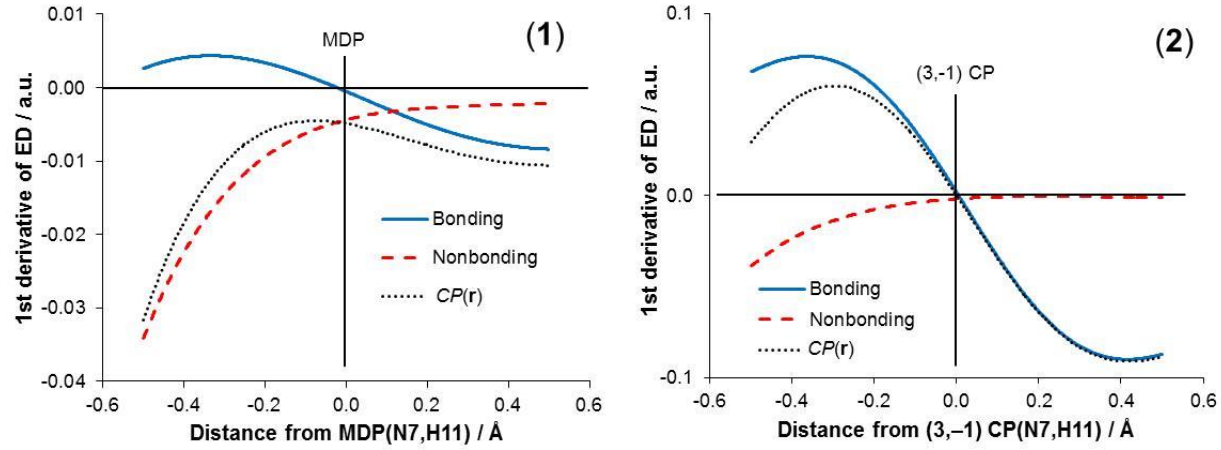

Figure 5. 1st derivative curves of the total *bonding*- and total *nonbonding*-ED as well as the *CP*(**r**) function computed along the λ_2–eigenvector passing through the MDP(N7,H11) in (**1**) and the (3,–1) CP(N7,H11) in (**2**).

As a matter of fact, the curves in Figure 5 serve as a nice and convenient pictorial representation of our *CP*(**r**) function computed along relevant λ_2–eigenvectors. Just as an example, see how slope of *bonding*-ED dominates that of *nonbonding*-ED in (**2**), thereby

meeting the criteria for the (3,–1) CP(N7,H11) and explaining the presence of the DB(N7,H11) in the protonated form of ethylenediamine.

Table 1. Selected contributions made to the MDP(N7,H11) in ethylenediamine. Percentages refer to contributions towards the *tot*-ED and its slope.

Component	$\rho_{bonding}(\mathbf{r^*})$	$\partial\rho_{bonding}(\mathbf{r^*})$	$\rho_{nonbonding}(\mathbf{r^*})$	$\partial\rho_{nonbonding}(\mathbf{r^*})$
N10,H11	0.00229 (20.7%)	0.00006 (1.0%)	-	-
N7,H9	0.00081 (7.3%)	0.00011 (1.8%)		
N7,H8	0.00060 (5.5%)	0.00002 (0.3%)		
N10,H12	0.00054 (4.9%)	-0.00027 (4.6%)	-	-
N7,H11	0.00053 (4.8%)	0.00003 (0.5%)	-	-
N7,N10	0.00030 (2.7%)	-0.00010 (1.6%)	-	-
C4,N7	-	-	0.00097 (8.8%)	-0.00090 (15.2%)
C1,N10	-	-	0.00079 (7.1%)	-0.00165 (27.9%)
C1,C4	-	-	0.00021 (1.9%)	-0.00081 (13.7%)
Total	**0.00826**	**-0.00042**	**0.00278**	**-0.00444**

Table 2. Selected contributions made to the (3,–1) CP(N7,H11) in protonated ethylenediamine. Percentages refer to contributions towards the *tot*-ED and its slope.

Component	$\rho_{bonding}(\mathbf{r^*})$	$\partial\rho_{bonding}(\mathbf{r^*})$	$\rho_{nonbonding}(\mathbf{r^*})$	$\partial\rho_{nonbonding}(\mathbf{r^*})$
N10,H11	0.00628 (16.5%)	-0.00156 (13.5%)	-	-
N7,H11	0.00537 (14.1%)	0.00122 (10.5%)		
N7,N10	0.00135 (3.6%)	0.00043 (3.7%)		
N10,H13	0.00096 (2.5%)	-0.00072 (6.2%)		
N10,H12	0.00085 (2.2%)	-0.00042 (3.6%)	-	-
N7,H9	0.00257 (6.8%)	0.00044 (3.8%)	-	-
N7,H8	0.00243 (6.4%)	0.00064 (5.5%)	-	-
C4,N7	0.00316 (8.3%)	-0.00093 (8.1%)	-	-
C1,N10	0.00115 (3.0%)	-0.00117 (10.1%)	-	-
C1,C4	-	-	0.00041 (1.1%)	-0.00003 (0.2%)
Total	**0.03743**	**0.00063**	**0.00056**	**0.00006**

Atom-pairs that made most significant contributions towards *tot*-ED at **r*** are included in Tables 1 and 2; a full set of data is included in Tables S7 and S8 in the SI. There are several important observations we would like to make:

(1) The atom-pair N7,H11 (H-bond acceptor and H-atom) involved in the primary interaction has not made the largest contribution to the ED at **r*** in both structures, (**1**) and (**2**), just 4.8 and 14.1% of the *tot*-ED, respectively. This is not entirely surprising, as we have noted similar observation in another case of a classical intramolecular H-bond.[27]

(2) The N10,H11 (H-bond donor and H-atom) atom-pair is the largest contributor to the *tot*-ED at **r*** in both structures, namely 20.7% and 16.5% in (**1**) and (**2**), respectively.

(3) The functional groups that essentially serve as a proton donor, $N10H_2$ in (**1**) and $N10H_3^+$ in (**2**), contributed most to the *tot*-ED in a bonding fashion, 25.6 and 21.2%, respectively.

(4) The $N7H_2$ functional groups that essentially serve as a proton acceptor in (**1**) and (**2**), made second largest *bonding*-ED contributions to the *tot*-ED, 12.8 and 9.4%, respectively.

(5) The nature of the contribution made by atom-pairs C1,N10 and C4,N7 changed from the largest *nonbonding*-ED component in (**1**) to a *bonding*-ED component in (**2**).

(6) In both structures, the strongest '*competing*' secondary interaction involving N7,N10 atom-pair has made constructive, hence a *bonding*-ED contribution of 2.7 and 3.6% in (**1**) and (**2**), respectively, to the *tot*-ED.

(7) There are numerous secondary interactions that contributed in a constructive manner to the *tot*-ED at **r***, *i.e.*, MDP(N7,H11) in (**1**) and (3,–1) CP(N7,H11) in (**2**); hence, they must not be seen as competing interactions.

The FALDI-based investigation reveals that a DB is a holistic, multicenter phenomenon[30] that, in the case of structures (**1**) and (**2**), involves the entire skeleton and both terminal functional groups (nearly entire molecules) in contributing to the ED in the internuclear region of the primary interaction. Furthermore, upon protonating (**1**), multiple atom-pairs either concentrated ED in a much stronger fashion, or concentrated ED in (**2**) even though they were depleting ED in the neutral structure. In this regard, the intramolecular interactions in (**1**) and (**2**) differ qualitatively: (i) physically, in that we expect stronger attractive forces to act on the N7, N10 and H11 nuclei due to increased ED concentration from multiple sources, and (ii) chemically, in that we expect greater constructive interference in the N7, N10 and H11 internuclear regions due to simultaneous MO overlap over a number of atomic basins. The MO overlap pattern is significantly different in (**1**) and (**2**) as well.

The added advantage of FALDI is in that makes it possible to extract contributions to the slope of the total *bonding*- and *nonbonding*-EDs in any structure. Analysis of data in Tables 1 and 2 reveals some surprising observations:

(a) There is no direct correlation between the ED contributed by an atom-pair to the primary interaction and this contribution's slope at r*; this observation equally applies to *bonding*- and *nonbonding*-ED contributions. Just as an example: (i) the largest *bonding*-ED contribution in (**1**) was made by N10,H11 (20.7% of the *tot*-ED), but this ED did not vary significantly in the proximity of MDP resulting in just 1% of the total slope at the

MDP(N7,H11); (ii) the largest *nonbonding*-ED contribution in (**1**) was made by C4,N7 but its slope at MDP(N7,H11) of 15.2% was largely 'outperformed' by the second largest *nonbonding*-ED contribution (C1,N10) that contributed 27.9 % to the slope of the total *nonbonding*-ED at MDP(N7,H11).

(b) The change (or slope) of *bonding*-ED contributions made by primary interactions in both structures at r* is not the most significant in terms of their contribution to the final slopes of the *tot*-ED. Hence, the primary interactions have no control over the presence or absence of a (3,–1) CP or DB in these two molecules.

(c) Finally, we note that the most significant in value secondary interaction between N7 and N10, constructively contributed to the internuclear region of the primary interaction in both structures, by adding ED and increasing the slope of *bonding*-ED. Clearly, this is not a competing interaction and this finding is in direct contrast to TJ's interpretation.[27,28]

Highly repulsive oxygen-oxygen interaction in similar organic molecules

The molecular graphs of two structurally similar organic structures, (**3**) and (**4**), are shown in Figure 6. The atom neighbouring C1 is different in these two equilibrium structures: element 2 in (**3**) is a F-atom and in (**4**), a H-atom. Atoms O6 and O8 of primary interaction (vdW radius of O = 1.52 Å) are not linked with a DB in (**3**), (d(O6,O8) = 2.8892 Å), but a DB is present in (**4**) (d(O6,O8) = 2.8838 Å).

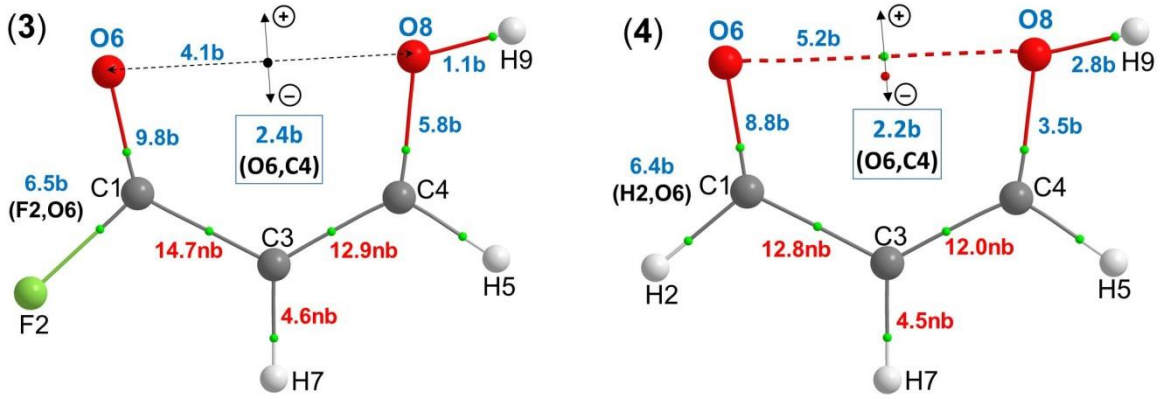

Figure 6. Molecular graphs of equilibrium structures of (**3**) and (**4**) in the gas phase also showing the directions of λ_2–eigenvectors crossing either the MDP(O6,O8) (black small sphere in (**3**)) or (3,–1) CP(O6,O8) on density bridge (green small sphere in (**4**)). Percentage-slope contributions made by atom-pairs that facilitate and hinder the presence of a DB(O6,O8) are shown as of bonding (b) and non-bonding (nb) nature, respectively.

There is no qualitative difference in the nature of the primary interaction from the IQA perspective as atoms O6 and O8 are involved in a highly repulsive and comparable in value interactions with $E_{\text{int}}^{\text{O6,O8}}$ in (**3**) and (**4**) of +125.8 and +120.4 kcal mol^{-1}, respectively. The

computed TJ's β-ratios,[27,28] $V_{XC}^{O6,O8}/V_{XC}^{O6,C4}$ of (–5.56)/(–3.42) = 1.63 for (**3**) and (–6.07)/(–4.29) = 1.41 for (**4**), yield very inconclusive results:

(a) Structure (**3**) has a β-ratio in the specified range in which a *primary* (3,–1) CP is predicted to be due to $\beta > 1.59$, but no DB is present.

(b) The trend of the β-ratio criterion does not hold for these molecules as, relative to (**3**), the smaller β-ratio in structure (**4**) does yield a DB.

This implies that either the DB(O6,O8) in (**4**) is of a different nature (*i.e.* not a "privileged exchange channel") or that the β-ratio does not represent an accurate criterion for the presence of a DB.

Figures 7(a) and 7(b) show the values and trends (along the λ_2–eigenvectors) computed for structures (**3**) and (**4**), respectively, shown in Figure 6. The *bonding*- and *nonbonding*-ED trends of the two structures are nearly identical, suggesting that the nature of the multicenter O6···O8 interaction in the two structures is highly comparable from an ED perspective.

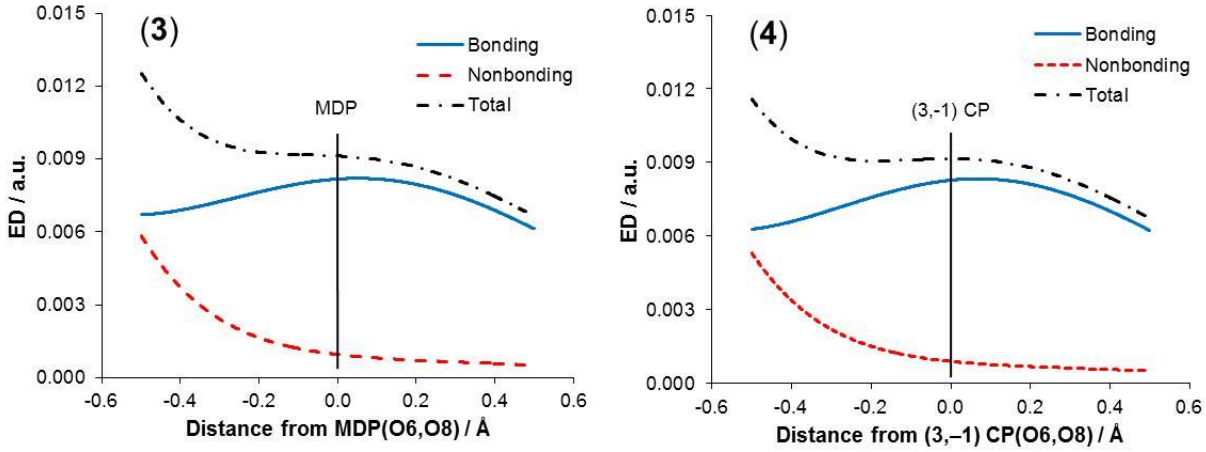

Figure 7. The *tot*-ED as well as the total *bonding*- and *nonbonding*-ED components computed along the λ_2–eigenvector passing through the MDP(O6,O8) in (**3**) and (3,–1) CP(O6,O8) in (**4**).

Figures 8(a) and 8(b) depict the gradients of the total *bonding*- and total *nonbonding*-ED values along the λ_2–eigenvectors in (**3**) and (**4**), respectively, as well as the *CP*(**r**) functions computed for both structures. *CP*(**r**) exhibits an almost identical shape for both structures, but is positive in a small region only in (**4**), where the slope of the *bonding*-ED is greater in magnitude than the slope of the *nonbonding*-ED. The rate of change of the *nonbonding*-ED is slightly smaller in magnitude in (**4**) than in (**3**), whereas the rate of change of *bonding*-ED is almost identical in both structures. However, this small difference results in a positive *CP*(**r**) in (**4**) and, hence, the presence of a DB.

We have also tested the *CP*(**r**) function's reliability at larger basis sets (aug-cc-pvqz), as shown in Section 3 of the SI. It is important to note that a DB between O atoms is absent in both (**3**) and (**4**) at this basis set and, correspondingly, our *CP*(**r**) function is negative throughout in both structures. This nicely illustrates sensitivity of the *CP*(**r**) function that was able to explain the presence/absence of a DB regardless of extremely small variations in topological differences generated by basis sets used in the calculations.

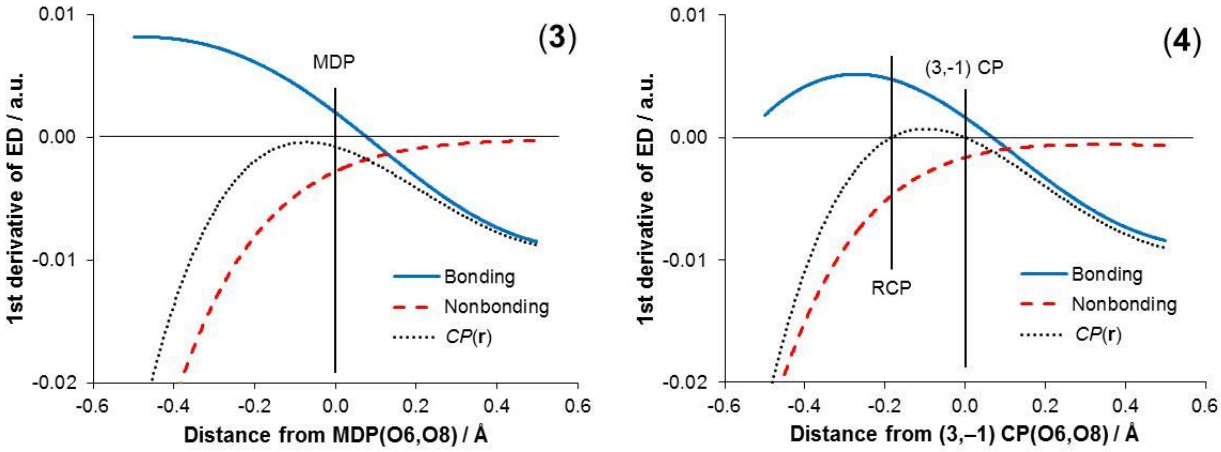

Figure 8. 1st derivative curves of the total *bonding*- and total *nonbonding*-ED as well as the *CP*(**r**) function computed along the λ_2–eigenvector passing through the MDP(O6,O8) in (**3**) and the (3,–1) CP(O6,O8) in (**4**).

Tables 3 and 4 show selected contributions in (**3**) and (**4**), respectively, to the *tot*-ED and its gradient at the MDP(O6,O8) and (3,–1) CP(O6,O8); a full set of data is included in Tables S9 and S10 in the SI. The most pertinent results from this comparison are:

(1) The ED delocalized between the atoms of the primary interaction (O6···O8, a repulsive, closed-shell interaction) is predominantly of a bonding nature in *both* (**3**) and (**4**), regardless of the presence or absence of a DB.

(2) Interestingly, there is no specific atom or atom-pair which is decisively responsible for the presence of a DB in (**4**) or absence of one in (**3**).

(3) Components that facilitate the presence of a DB between O6 and O8 are generally from the neighbouring atoms, whereas the carbon backbone generally hinders DB presence.

(4) The atom-pair O6,O8 involved in the primary interaction has not made the largest contribution to the ED at **r*** in *both* (**3**) and (**4**), just 7.1 and 7.7% of the *tot*-ED, respectively.

(5) Interactions that might be interpreted as '*competing*' (such as C4···O6) in fact facilitate the presence of a DB between O6 and O8.

(6) The C1,O6 atom-pair is the largest contributor to the *tot*-ED at **r*** in both structures, namely 15.2 and 13.4% in (**3**) and (**4**), respectively.

(7) The factors that hinder or facilitate the presence of a DB(O6,O8) in (**4**) are the same as in (**3**).

(8) Numerous small differences in the magnitudes of the various factors' contributions are such that the slope of the *nonbonding*-ED in (**3**) is slightly greater than in (**4**), and as a result, a DB doesn't appear in (**3**).

Table 3. Selected contributions made to the MDP(O6,O8) in (**3**). Percentages refer to contributions towards the *tot*-ED and its slope.

Component	$\rho_{\text{bonding}}(\mathbf{r^*})$	$\partial\rho_{\text{bonding}}(\mathbf{r^*})$	$\rho_{\text{nonbonding}}(\mathbf{r^*})$	$\partial\rho_{\text{nonbonding}}(\mathbf{r^*})$
C1,O6	0.00138 (15.2%)	-0.00048 (9.8%)	-	-
O6,O8	0.00065 (7.1%)	0.00020 (4.1%)	-	-
C4,O6	0.00024 (2.7%)	0.00012 (2.4%)	-	-
O6 loc	0.00021 (2.3%)	0.00046 (9.4%)	-	-
C1,C3	-	-	0.00023 (2.5%)	-0.00072 (14.7%)
C3,C4	-	-	0.00022 (2.4%)	-0.00064 (12.9%)
Total	**0.00818**	**0.00114**	**0.00094**	**-0.00189**

Table 4. Selected contributions made to the (3,–1) CP(O6,O8) in (**4**). Percentages refer to contributions towards the *tot*-ED and its slope.

Component	$\rho_{\text{bonding}}(\mathbf{r^*})$	$\partial\rho_{\text{bonding}}(\mathbf{r^*})$	$\rho_{\text{nonbonding}}(\mathbf{r^*})$	$\partial\rho_{\text{nonbonding}}(\mathbf{r^*})$
C1,O6	0.00123 (13.4%)	-0.00041 (8.8%)	-	-
O6,O8	0.00071 (7.7%)	0.00024 (5.2%)	-	-
C4,O6	0.00027 (3.0%)	0.00010 (2.2%)	-	-
O6 loc	0.00021 (2.3%)	0.00039 (8.5%)	-	-
C1,C3	-	-	0.00022 (2.4%)	-0.00060 (12.8%)
C3,C4	-	-	0.00022 (2.4%)	-0.00056 (12.0%)
Total	**0.00828**	**0.00173**	**0.00087**	**-0.00168**

The above analyses of *bonding*- and *nonbonding*-ED distributions (Figure 7) and their slopes (Figure 8) as well as the IQA-defined interaction energies show that the physical nature of the two multicentre O6···O8 interactions is fundamentally the same. However, the *bonding*-ED contribution at the (3,–1) CP(O6,O8) in (**4**) is slightly larger than at MDP(O6,O8) in (**3**) (0.00071 and 0.00065 a.u., respectively) as well as its rate of change along the λ_2-eigenvector. Therefore, we expect that the attractive forces acting on the nuclei to be greater in (**4**) than in (**3**) – a statement corroborated by a slightly less repulsive IQA interaction energy, by 5.4 kcal·mol^{-1} in (**4**). From a chemical point of view, we expect increased constructive interference from MO overlap across both O6 and O8 atomic basins – again, corroborated by slightly greater $V_{\text{XC}}^{\text{O6,O8}}$ term of the interaction energy, by 0.5 kcal·mol^{-1}) in (**4**). Furthermore and importantly, our analysis shows that the ED in the internuclear region is of multicenter nature; hence, all contributions need to be taken into

account in order to fully understand this interaction in both molecules. This is possibly why TJ's β-ratio fails to correctly predict the DB(O6,O8) in (**4**).

In summary and to conclude, the total *bonding*-ED (as well as its rate of change) increases from (**3**) to (**4**), whilst the total *nonbonding*-ED (as well as its rate of change) decreases in magnitude from (**3**) to (**4**). Therefore, it seems likely that the multicenter intramolecular O6···O8 interaction is slightly less repulsive in (**4**) than in (**3**) (from both physical and chemical points of view), due to manner in which ED is distributed. The consequence of these changes is the presence of a DB in (**4**). However, the changes between (**3**) and (**4**) are extremely small, and this case study clearly demonstrates that a DB can appear due to almost insignificant changes that have no bearing on the overall interpretation of an interaction on a fundamental level.

Attractive chlorine-chlorine interaction in di- and hexa-chloroethane

The third case study involves the comparison of a Cl···Cl interaction in eclipsed conformations (non-equilibrium structures) of chlorine-substituted ethane. The molecular graphs of di- and hexachloroethane ($C_2H_4Cl_2$ (**5**) and C_2Cl_6 (**6**)) in Figure 9 show that a DB is present between each pair of eclipsed chlorine atoms only in (**6**).

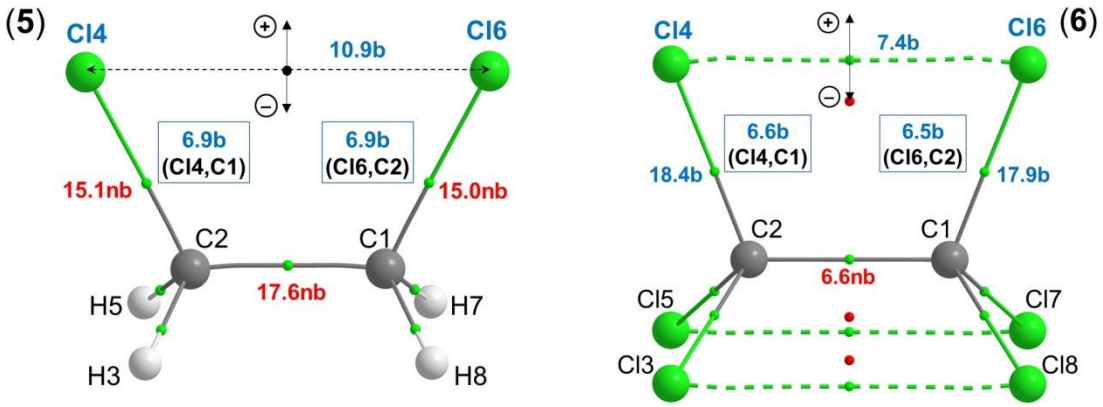

Figure 9. Molecular graphs of eclipsed $C_2H_4Cl_2$ (**5**) and C_2Cl_6 (**6**) structures in the gas phase also showing the directions of λ_2–eigenvectors crossing either the MDP(Cl4,Cl6) (black small sphere in (**5**)) or (3,–1) CP(Cl4,Cl6) on a density bridge (green small sphere in (**6**)). Percentage-slope contributions made by atom-pairs that facilitate and hinder the presence of a DB(Cl4,Cl6) are shown as of bonding (b) and non-bonding (nb) nature, respectively.

The interaction between Cl4 and Cl6 atoms in both structures is characterised by rather small in value, repulsive in nature classical term that is compensated over by the $V_{XC}^{Cl4,Cl6}$ term. As a result, these atoms are involved in an overall attractive interactions, with $E_{int}^{Cl4,Cl6}$ = –5.29 kcal mol^{-1} ($V_{XC}^{Cl4,Cl6}$ = –9.87 kcal mol^{-1}) in (**5**) and $E_{int}^{Cl4,Cl6}$ = –12.34 kcal mol^{-1} ($V_{XC}^{Cl4,Cl6}$ =

–13.70 kcal mol^{-1}) in (**6**) even though one can see them as being involved in a steric clash as d(Cl4,Cl6) = 3.2142 and 3.0196 Å, respectively, in (**5**) and (**6**) (vdW radius of Cl = 1.75 Å).

The computed TJ's β-ratios,[27,28] $V_{XC}^{Cl4,Cl6}/V_{XC}^{Cl4,C1}$ of (–9.87)/(–5.06) = 1.95 for (**5**) and (–13.70)/(–4.79) = 2.86 for (**6**), are both larger than the specified upper limit value of 1.59; hence the β-ratio incorrectly predicts a DB linking Cl4 with Cl6 in both structures. Furthermore, $V_{XC}^{Cl4,Cl6}$ in (**5**) is almost twice as large as that of the largest secondary interaction, and therefore this interaction is considered privileged in such a context, yet no DB is present. This must raise some questions regarding the arbitrariness of TJ's interpretation of Pendás *et al.*'s concept of privileged exchange channels.[26]

Figures 10(a) and 10(b) show the FALDI-based ED decomposition of the total *bonding*- and *nonbonding*-ED along the λ_2–eigenvectors indicated in Figure 9. In this case study we see some very large differences in the ED distributions. While the *tot*-ED distributions in the vicinity of the MDP(Cl4,Cl6) in (**5**) and (3,–1) CP(Cl4,Cl6) in (**6**) are comparable in magnitude, the ratio of *bonding*- to *nonbonding*-ED in (**6**) is much larger. Furthermore, we note in (**5**) that *nonbonding*-ED dominates the negative range of the eigenvector (a direction 'towards' the carbon backbone) whereas in (**6**) it makes rather small (nearly negligible) contribution throughout entire region.

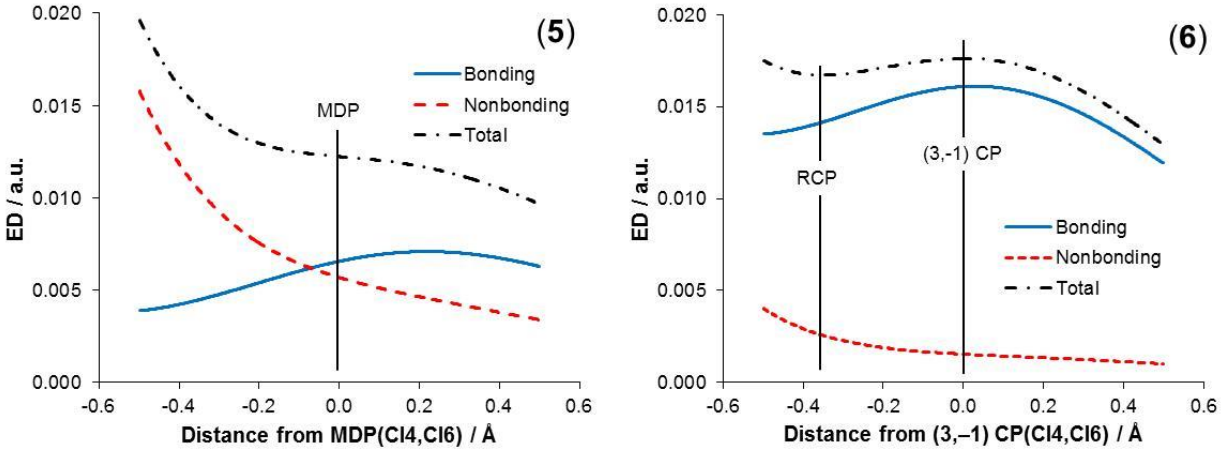

Figure 10. The *tot*-ED as well as the total *bonding*- and *nonbonding*-ED components computed along the λ_2–eigenvector passing through the MDP(Cl4,Cl6) in (**5**) and (3,–1) CP(Cl4,Cl6) in (**6**).

Slopes of the total *bonding*- and total *nonbonding*-ED distributions, as well as the *CP*(**r**) function, with respect to the λ_2–eigenvector, are plotted in Figures 11(a) and 11(b). The criterion and mechanism leading to a DB existence using the *CP*(**r**) function once again holds, in that *CP*(**r**) is always negative between Cl4 and Cl6 atoms in (**5**) but displays a

positive region in (**6**). This provides an evidence that the *CP*(**r**) function is equally applicable and successful in its predictive ability for either equilibrium or non-equilibrium structures.

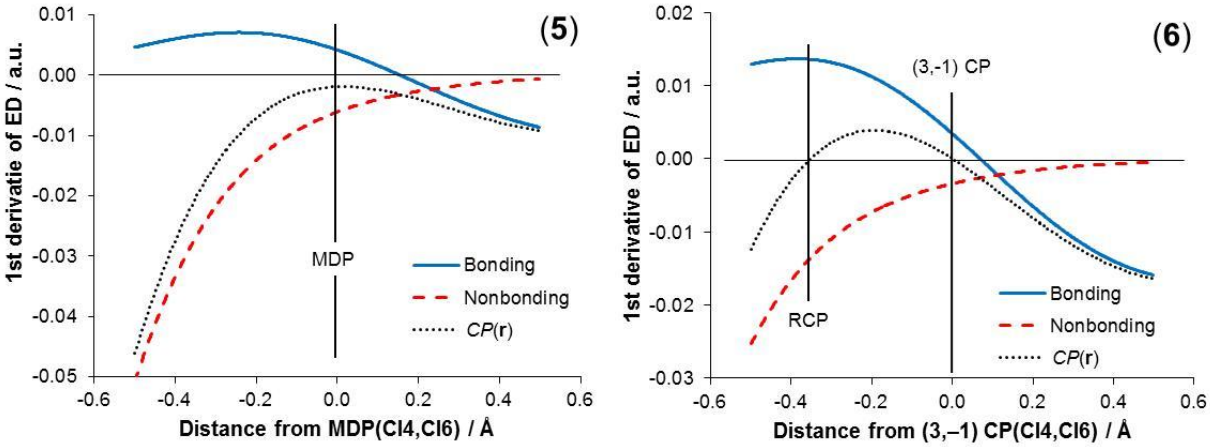

Figure 11. 1st derivative curves of the total *bonding*- and total *nonbonding*-ED as well as the *CP*(**r**) function computed along the λ_2–eigenvector passing through the MDP(Cl4,Cl6) in (**5**) and the (3,–1) CP(Cl4,Cl6) in (**6**).

The substitution of H-atoms in (**5**) for Cl atoms in (**6**) has a very significant influence on the *bonding*- and *nonbonding*-ED distributions, as well as their slopes, between Cl-atoms. The largest contributions are shown in Tables 5 and 6; a full set of data is included in Tables S11 and S12 in the SI. There are several important observations we would like to make:

(1) In contrast to previous molecules, the atom-pair Cl4,Cl6 involved in the primary interaction made the largest contribution to the ED at **r*** in both structures (**5**) and (**6**), 14.9 and 12.3% of the *tot*-ED, respectively.

(2) Atom-pairs C1,C2 and C2,Cl4 hinder DB(Cl4,Cl6) presence in (**5**) (on average by ~16% of the total slope, nonbonding) but C2,Cl4 facilitates DB(Cl4,Cl6) presence in (**6**) (~18% of total slope, bonding) whereas C1,C2 atom-pair's *nonbonding*-ED contribution decreased by about 50%.

(3) Long-range Cl···Cl interactions present in (**6**), such as from the atom-pair Cl3,Cl4, facilitate the presence of DBs between eclipsed Cl-atoms. Each of the long-range Cl···Cl interaction contributes ~3.7% to the total slope at the (3,–1) CPs in a bonding fashion; in total, they contribute ~24% to the total slope and ~35% to the *tot*-ED at, *e.g.* the (3,–1) CP(Cl4,Cl6).

(4) The ED delocalized amongst various Cl atom-pairs (both eclipsed and non-eclipsed) is therefore distributed in a manner that *concentrates* ED between *all* eclipsed Cl···Cl contacts, as a result of molecular-wide MOs that show constructive interference between neighbouring Cl atoms.

Table 5. Selected contributions made to the MDP(Cl4,Cl6) in (**5**). Percentages refer to contributions towards the *tot*-ED and its slope.

Component	$\rho_{bonding}(\mathbf{r^*})$	$\partial\rho_{bonding}(\mathbf{r^*})$	$\rho_{nonbonding}(\mathbf{r^*})$	$\partial\rho_{nonbonding}(\mathbf{r^*})$
Cl4,Cl6	0.00182 (14.9%)	0.00122 (10.9%)	-	-
C1,Cl4	0.00085 (6.9%)	0.00078 (6.9%)	-	-
C2,Cl4	-	-	0.00176 (14.4%)	-0.00169 (15.1%)
C1,C2	-	-	0.00053 (4.3%)	-0.00197 (17.6%)
Total	**0.00658**	**0.00465**	**0.00563**	**-0.00653**

Table 6. Selected contributions made to the (3,–1) CP(Cl4,Cl6) in structure (**6**). Percentages refer to contributions towards the *tot*-ED and its slope.

Component	$\rho_{bonding}(\mathbf{r^*})$	$\partial\rho_{bonding}(\mathbf{r^*})$	$\rho_{nonbonding}(\mathbf{r^*})$	$\partial\rho_{nonbonding}(\mathbf{r^*})$
Cl4,Cl6	0.00218 (12.3%)	0.00066 (7.4%)	-	-
C1,Cl4	0.00095 (5.4%)	0.00058 (6.6%)	-	-
C2,Cl4	0.00193 (10.9%)	-0.00163 (18.4%)	-	-
Cl3,Cl4	0.000991 (5.6%)	0.000328 (3.7%)		
C1,C2	-	-	0.00041 (2.3%)	-0.00058 (6.6%)
Total	**0.01611**	**0.00153**	**0.00129**	**-0.00115**

Clearly, from the MOs perspective, interactions between eclipsed Cl-atoms in (**5**) and (**6**) might be seen as distinctively different even though, from the IQA perspective, they are nearly identical. It is therefore not the Cl···Cl interaction itself which is different between the two structures, but rather a remarkably different environment in (**6**) which leads to a predominantly multicenter interaction involving considerable *bonding*-ED contributions. These additional *bonding*-ED contributions in (**6**) result in a relative increase in the slope of the factors that concentrate ED in the Cl4,Cl6 internuclear region, and as a result, a DB(Cl4,Cl6) is observed.

Although this work is focused on intramolecular interactions, following the reviewer's suggestion, we have also applied our protocol to the 'classical' C–C bond in (**6**). As one would expect, the *CP*(**r**) function worked perfectly well also in this case and was (i) positive in the vicinity of the (3,–1) CP(C1,C2) and (ii) equal to zero at this CP. Interestingly, the *tot*-ED was made-up entirely of *bonding*-ED component in this case. Furthermore, as reported recently for "linear" *n*-butane,[30] the largest but not exclusive contributor to the *tot*-ED is the ED delocalized between the atoms of the primary contribution – atom-pair C1,C2 contributed 47.6% to the total ED at the (3,–1) CP(C1,C2); note that ~52 % (majority) of the ED at the (3,–1) CP(C1,C2) comes from numerous contributions made by other atom-pairs in the C_2Cl_6 molecule. This confirmed again that even 'classical' covalent bonds show large degree of multicentre nature of bonding; interested readers are referred to Section 4 in the SI for more details.

H--H steric contact in *cis*-2-butene

Finally, as requested by another reviewer, analysis of the H--H steric contact, with d(H1,H6) = 2.1150 Å < sum of vdW radii, in *cis*-2-butene was performed using exactly the same approach as discussed for the remaining molecular systems – the molecular graph and λ_2–eigenvector are shown in Figure 1(a). The reviewer's suggestion clearly stemmed from the fact that the so-called hydrogen–hydrogen bonds, citing the reviewer, 'have been plaguing the QTAIM paradigm for a while'. Furthermore, from NBO-based analysis it was concluded[42] recently that the H···H interaction in the *cis*-isomer of 2-butene is repulsive and responsible for this conformer higher energy relative to the *trans*-conformer (the equilibrium structure).

Looking at trends shown in Figure 12, however, it is apparent that the presence of a DB

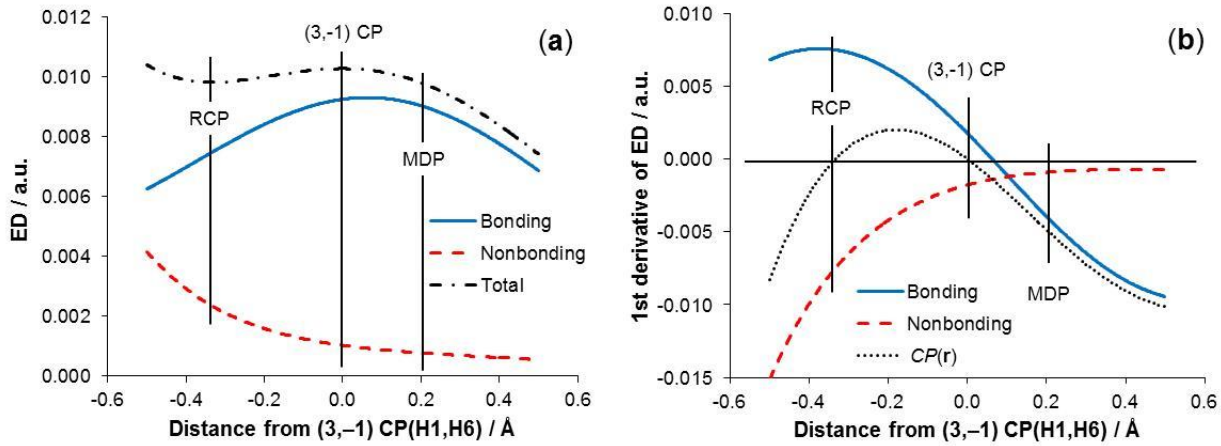

Figure 12. Part (a) - the *tot*-ED and its components, the total *bonding*- and *nonbonding*-ED, and part (b) - the 1st derivative curves of the total *bonding*- and *nonbonding*-ED components and the *CP*(**r**) function computed for both parts along the λ_2–eigenvector passing through the (3,–1) CP(H1,H6) in *cis*-2-butene. RCP ((3,+1) CP) and (3,–1) CP occur when *CP*(**r**) = 0.

and the associated (3,–1) CP(H1,H6) is the result of the same fundamental processes that lead to DBs in molecules discussed above:

a) The *tot*-ED peaks at the (3,–1) CP and, most importantly, is largely dominated by bonding contributions as depicted in Figure 12(a). Notably, the H1 and H6 atoms (as well as the CH1···H6C fragment) are involved, relative to the equilibrium structure, *i.e.*, *trans*-2-butene, in more attractive IQA-defined intrafragment interactions.[43]

b) The *CP*(**r**) function is positive in the region between RCP and (3,–1) CP(H1,H6) (Figure 12(b)) and this is a result of the larger slope computed for the *bonding*-ED relative to *nonbonding*-ED – see data in Table 7 where major %-contributions towards the *tot*-ED and its slope are presented. Clearly, *CP*(**r**) > 0 is always observed between the two topological points

for intramolecular interactions characterised by the presence of a DB regardless whether atoms are involved in attractive or repulsive interaction.

c) The MDP is located in Figure 12(b) in the region where the *CP*(**r**) function is negative and this is also observed for other molecules investigated regardless whether without or with the (3,–1) CP, hence a DB.

Table 7. Selected contributions made to the (3,–1) CP(H1,H6) in *cis*–2–butene. Percentages refer to contributions towards the *tot*-ED and its slope.

Component	$\rho_{\text{bonding}}(\mathbf{r}^*)$	$\partial\rho_{\text{bonding}}(\mathbf{r}^*)$	$\rho_{\text{nonbonding}}(\mathbf{r}^*)$	$\partial\rho_{\text{nonbonding}}(\mathbf{r}^*)$
C2,H1	0.00268 (26.1%)	0.00066 (16.3%)	-	-
C5,H6	0.00268 (26.1%)	0.00066 (16.3%)		
H1,H6	0.00030 (2.9%)	0.00007 (1.7%)		
C2,H7	0.00031 (3.1%)	-0.00004 (0.9%)	-	-
C2,C3	-	-	0.00032 (3.1%)	-0.00061 (14.9%)
C4,C5	-	-	0.00032 (3.1%)	-0.00061 (14.9%)
C3,C4	-	-	0.00010 (1.0%)	-0.00029 (7.1%)
C3,H12	-	-	0.00003 (0.3%)	-0.00007 (1.8%)
Total	**0.00925**	**0.00178**	**0.00103**	**-0.00178**

Data in Table 7 provides further and important insight when atom-pairs' main contributions are considered:

1) The largest contributions of a bonding nature came from C2,H1 (C5,H6) atom pairs (0.00268 a.u. each and when combined it constitutes 52.2 % of the *tot*-ED) that is an order of magnitude larger when compared with contribution (also of *bonding* nature) made by the H1,H6 atom-pair involved in steric 'clash'. This (i) correlates perfectly well with these two fragments being stabilized in *cis*-2-butene relative to the *trans*-conformer[43] as *loc*-FAMSEC < 0 (FAMSEC = Fragment Attributed Molecular System Energy Change[44]) and (ii) strongly suggests that a four-atom notation, CH···HC, for this kind of interaction is most representative.

2) Major contributions of nonbonding nature came from atom-pairs of the molecular backbone, among them the middle C3,C4 atom pair that became somewhat strained when in *cis*-conformer.[43]

Conclusions

A set of analytical quantum chemical tools was developed in order to study and understand the presence or absence of a density bridge (DB) linking two atoms on a molecular graph. Applicability and usefulness of the tools was successfully tested on four very different case

studies involving intramolecular interactions: (1) a classical H-bond, (2) a highly repulsive O···O interaction, (3) an attractive Cl···Cl interaction and (4) DB-linked an attractive CH···HC interaction. The first three case studies involved two similar molecules showing either an absence or presence of a DB.

We have consistently shown that the presence or absence of a DB cannot be linked to the *β*-ratio of IQA-defined $V_{\mathrm{XC}}^{\mathrm{X,Y}}$ terms of the interaction of interest (the so-called '*primary interaction*') and the '*competing*' neighbouring interactions ('*secondary interactions*').[27,28] Rather, we showed that all of the DBs studied in this work displayed very large degree of multicenter character, illustrating that a simple bicentric approach for introducing a criterion for the presence of a DB represents a grossly misleading picture of the topology of the ED. In fact, in all four systems studied in this work, the atom-pair of the intramolecular interactions that display a DB only contributed a relatively small fraction of the *tot*-ED as well as its slope at the (3,–1) CP. While Pendás *et al*'s concept of DBs as "privileged exchange channels"[26] might still hold, it must be redefined within a framework of multiple exchange channels resulting in a single density bridge.

Using the FALDI-based ED decomposition scheme, we have shown that for a specific internuclear region, multiple atoms and atom-pairs can either facilitate or hinder the presence of a DB due to the manner in which (de)localized ED is distributed across the molecule. We have labelled each component as bonding, nonbonding or antibonding, related to each components' partial second derivative along the λ_2-eigenvector. In all of our model systems we noticed multiple, often unexpected bonding or nonbonding contributions to an internuclear region of interest. For instance, (i) multiple Cl,Cl atom-pairs *facilitate* the presence of DBs between eclipsed Cl,Cl contacts in hexachloroethane (**6**), a factor which is missing in dichloroethane (**5**) or (ii) the two CH fragments of the bay in *cis*-2-butene contributed in bonding fashion to the interatomic region between H-atoms involved in the steric contact most and an order of magnitude more than clashing H-atoms that also contributed to the total *bonding*-ED. Ultimately, we showed that the relative slopes (rates of change) of *bonding*-, *nonbonding*- and *antibonding*-ED determines the presence of a DB, and in the absence of *antibonding*-ED, a DB will always exist if the slope of the *bonding*-ED is greater in magnitude than the slope of the *nonbonding*-ED in a given internuclear region. Since each FALDI component can be interpreted from a physical (*i.e.* in terms of the forces acting on nuclei) and chemical (*i.e.* in terms of interference patterns of MOs overlapping multiple atoms) points of view, we present a criterion that provides a very useful and descriptive language for interpreting QTAIM's molecular graphs.

Analysis of the ED distributions of our model systems revealed that many contributions of a bonding nature are present regardless of whether a primary interaction is (i) linked by a DB (ii) repulsive or attractive, and/or (iii) considered as chemically bonded. As such, we cannot suggest using the presence of a DB as a condition for any chemical phenomenon. That said, the presence of a DB proves that some ED contributions in an internuclear region are of a bonding nature; hence any (multicenter) interaction with a DB present displays a degree of bonding character, thereby strengthening or weakening attractive or repulsive interatomic forces, respectively.

Our observations point towards a necessary paradigm shift in the relationship between ED distributions in internuclear regions and chemical bonding, especially for the description of intramolecular interactions. While we hope, as many chemical theoreticians do, for the discovery of a universal, general theory of the chemical bond, we suggest that, perhaps, it is necessary to fully understand the inherently multicenter characteristics of bonding, nonbonding and antibonding in terms of ED distributions first, regardless of whether a chemical interaction can ultimately be considered as bonded or not.

Acknowledgements

This work is based on the research supported in part by the National Research Foundation of South Africa (Grant Number 105855). The authors gratefully acknowledge the Centre for High Performance Computing (CHPC), South Africa, for providing computational resources to this research project.

The authors declare no conflict of interest.

References

[1] The Chemical Bond: Chemical Bonding Across the Periodic Table; G. Frenking, S. Shaik, Eds.; Wiley-VCH: Weinheim, **2014**.

[2] The chemical bond: fundamental aspects of chemical bonding; The Chemical Bond: Chemical Bonding Across the Periodic Table; G. Frenking, S. Shaik, Eds.; Wiley-VCH: Weinheim, **2014**.

[3] P. L. Popelier, In The Chemical Bond II; D. Mingos, Ed.; Springer:Cham, **2016**; Vol. 170, p 71-117.

[4] R. F. W. Bader, In Atoms in molecules: A Quantum Theory; Oxford University Press: Oxford, **1990**.

[5] C. Foroutan-Nejad, S. Shahbazian, R. Marek, *Chem. Eur. J*. **2014**, *20*, 10140–10152.

[6] S. Shahbazian, *Chem. Eur. J.* **2018**, *24*, 5401–5405.

[7] G. Runtz, R. F. W. Bader, R. Messer, *Can. J. Chem.* **1977**, *55*, 3040–3045.

[8] R. F. W. Bader, T. H. Tang, Y. Tal, F. W. Biegler-Koenig, *J. Am. Chem. Soc.* **1982**, *104*, 946–952.

[9] S. Grimme, C. Mück-Lichtenfeld, G. Erker, G. Kehr, H. Wang, H. Beckers, H. Willner, *Angew. Chem. Int. Ed* **2009**, *48*, 2592–2595.

[10] A. Krapp, G. Frenking, *Chem. Eur. J.* **2007**, *13*, 8256–8270.

[11] J. Poater, M. Solà, F. M. Bickelhaupt, *Chem. Eur. J.* **2006**, *12*, 2889–2895.

[12] J. Poater, M. Solà, F. M. Bickelhaupt, *Chem. Eur. J.* **2006**, *12*, 2902–2905.

[13] J. Poater, R. Visser, M. Solà, F. M. Bickelhaupt, *J. Org. Chem.* **2007**, *72*, 1134–1142.

[14] I. Cukrowski, J. H. de Lange, A. S. Adeyinka, P. Mangondo, *Comput. Theor. Chem.* **2015**, *1053*, 60–76.

[15] R. F. W. Bader, *J. Phys. Chem. A* **2009**, *113*, 10391–10396.

[16] R. F. W. Bader, *J. Phys. Chem. A* **1998**, *102*, 7314–7323.

[17] D. Cremer, E. Kraka, *Croat. Chem. Acta* **1985**, *57*, 1259–1281.

[18] R. F. W. Bader, T. Slee, D. Cremer, E. Kraka, *J. Am. Chem. Soc.* **1983**, *105*, 5061–5068.

[19] L. J. Farrugia, C. Evans, M. Tegel, *J. Phys. Chem. A* **2006**, *110*, 7952–7961.

[20] J. R. Lane, J. Contreras-García, J.-P. Piquemal, B. J. Miller, H. G. Kjaergaard, *J. Chem. Theory Comput.* **2013**, *9*, 3263–3266.

[21] C. F. Matta, J. Hernández-Trujillo, T. H. Tang, R. F. W. Bader, *Chem. Eur. J.* **2003**, *9*, 1940–1951.

[22] R. F. W. Bader, *Chem. Eur. J.* **2006**, *12*, 2896–2901.

[23] J. Contreras-García, E. R. Johnson, S. Keinan, R. Chaudret, J.-P. Piquemal, D. N. Beratan, W. Yang, *J. Chem. Theory Comput.* **2011**, *7*, 625–632.

[24] A. Otero-de-la-Roza, E. R. Johnson, J. Contreras-García, *Phys. Chem. Chem. Phys.* **2012**, *14*, 12165–12172.

[25] R. F. W. Bader, *Can. J. Chem.* **1986**, *64*, 1036–1045.

[26] A. M. Pendás, E. Francisco, M. A. Blanco, C. Gatti, *Chem. Eur. J.* **2007**, *13*, 9362–9371.

[27] O. A. Syzgantseva, V. Tognetti, L. Joubert, *J. Phys. Chem. A* **2013**, *117*, 8969–8980.

[28] V. Tognetti, L. Joubert, *J. Chem. Phys.* **2013**, *138*, 024102–024111.

[29] M. Blanco, A. M. Pendás, E. Francisco, *J. Chem. Theory Comput.* **2005**, *1*, 1096–1109.

[30] J. H. de Lange, D. M. van Niekerk, I. Cukrowski, *J. Comput. Chem* **2018**, *39*, 973–985.

[31] R. P. Feynman, *Phys. Rev.* **1939**, *56*, 340–343.

[32] J. H. Lange, I. Cukrowski, *J. Comput. Chem.* **2017**, *38*, 981–997.

[33] I. Cukrowski, D. M. van Niekerk, J. H. de Lange, *Struct. Chem.* **2017**, *28*, 1429–1444.

[34] J. H. de Lange, I. Cukrowski, *J. Comput. Chem.* **2018**, *DOI: 10.1002/jcc.25223*.

[35] R. Ponec, *J. Math. Chem.* **1997**, *21*, 323–333.

[36] R. Ponec, *J. Math. Chem.* **1998**, *23*, 85–103.

[37] M. Frisch, G. Trucks, H. Schlegel, G. Scuseria, M. Robb, J. Cheeseman, G. Scalmani, V. Barone, B. Mennucci, G. Petersson, H. Nakatsuji, X. Li, M. Caricato, A. Marenich, J. Bloino, B. Janesko, R. Gomperts, B. Mennucci, H. Hratchian, J. Ortiz, A. Izmaylov, J. Sonnenberg, D. Williams-Young, F. Ding, F. Lipparini, F. Egidi, J. Goings, B. Peng, A. Petrone, T. Henderson, D. Ranasinghe, V. Zakrzewski, J. Gao, N. Rega, G. Zheng, W. Liang, M. Hada, M. Ehara, K. Toyota, R. Fukuda, J. Hasegawa, M. Ishida, T. Nakajima, Y. Honda, O. Kitao, H. Nakai, T. Vreven, K. Throssell, J. J. Montgomery, J. Peralta, F. Ogliaro, M. Bearpark, J. Heyd, E. Brothers, K. Kudin, V. Staroverov, T. Keith, R. Kobayashi, J. Normand, K. Raghavachari, A. Rendell, J. Burant, S. Iyengar, J. Tomasi, M. Cossi, J. Millam, M. Klene, C. Adamo, R. Cammi, J. Ochterski, R. Martin, K. Morokuma, O. Farkas, J. Foresman, D. Fox, Gaussian, Inc., Wallingford CT, **2009**.

[38] S. Grimme, *Wiley Interdiscip. Rev. Comput. Mol. Sci.* **2011**, *1*, 211–228.

[39] T. Keith, TK Gristmill Software (aim.tkgristmill.com): Overland Parks KS, USA, **2016**.

[40] W. Humphrey, A. Dalke, K. Schulten, *J. Mol Graph.* **1996**, *14*, 33–38.

[41] A. Bondi, *J. Phys. Chem.* **1964**, *68*, 441–451.

[42] F. Weinhold, P. R. Schleyer, W. C. McKee, *J. Comput. Chem.* **2014**, *35*, 1499–1508.

[43] I. Cukrowski, F. Sagan, M. P. Mitoraj, *J. Comput. Chem.* **2016**, *37*, 2783–2798.

[44] I. Cukrowski, *Comput. Theor. Chem*. **2015**, *1066* (2015) 62–75.